2003

Constraint preserving boundary conditions for the linearized Einstein equations

Gioel Calabrese
Louisiana State University and Agricultural and Mechanical College

CONSTRAINT PRESERVING BOUNDARY CONDITIONS FOR THE LINEARIZED EINSTEIN EQUATIONS

A Dissertation

Submitted to the Graduate Faculty of the
Louisiana State University and
Agricultural and Mechanical College
in partial fulfillment of the
requirements for the degree of
Doctor of Philosophy

in

The Department of Physics and Astronomy

by
Gioel Calabrese
B.S., University of Parma, 1999
December 2003

To my family, for their love and support.

Acknowledgments

I would like first and foremost to thank my advisor Dr. Jorge Pullin for creating a stimulating and challenging research environment. I would also like to thank Dr. Luis Lehner, Dr. Joseph Giaime and Dr. Joel Tohline from the Department of Physics and Astronomy and Dr. Michael Tom from the Department of Mathematics for serving on my dissertation committee.

My work here has been supported in part by the Economic Development Assistantship and by the Charles E. Coates Fellowship. The computational aspect of the dissertation relies heavily on technology provided by LSU. I am also grateful to the assistance of the Physics Department staff, particularly Arnell Dangerfield, Karen Richard, and Robert Dufrene and to a fellow graduate student, Shangli Ou, for his help with visualization. I would also like to extend my thanks to members, past and present, of the Department of Physics and Astronomy at The Pennsylvania State University, where my graduate studies began and where I was first introduced to the field of numerical relativity.

Many people have added to my experience of graduate studies over the past four years and, although they may not have contributed directly to this work, I owe them my thanks for their time, support and guidance. Among them is Dr. Oscar Reula of the University of Córdoba, with whom I had many pleasant discussions and from whom I have learned a lot. I am also grateful to members of the various institutions where I have spent time as a guest, including Caltech, the University of Parma, the Max-Planck-Institut für Gravitationsphysik, the University of Southampton, SISSA, the University of Utah, and the University of Wisconsin-Milwaukee.

I would like to thank my fellow members of the General Relativity Theory Group at LSU. I am indebted to Dr. Olivier Sarbach, who has always been so generous in sharing his time, thoughts and knowledge with me. I wish to thank Dr. David Neilsen for one of the most enjoyable collaborative projects of my doctoral years. I am very happy to have had the opportunity to meet him and his family. I also thank Dr. Luis Lehner for providing direction and advice, Dr. Manuel Tiglio and Dr. Jason Ventrella.

Finally I would like to thank members of my family for their support and encouragement. My wife, Pamela, has literally crossed oceans for my pursuit of graduate studies and has been a great source of strength to me. I thank my parents for their support and lively interest in my academic endeavors.

Table of Contents

Abstract

The successful construction of long time convergent finite difference schemes approximating highly gravitating systems in general relativity remains an elusive task. The presence of constraints and the introduction of artificial time-like boundaries contribute significantly to the difficulty of this problem. Whereas in the absence of boundaries the Bianchi identities ensure that the constraints vanish during evolution provided that they are satisfied initially, this is no longer true when time-like boundaries are introduced. In this work we consider the linearization around the Minkowski space-time in Cartesian coordinates of the generalized Einstein-Christoffel system and analyze different kinds of boundary conditions that are designed to ensure that the constraints vanish throughout the computational domain: the Neumann, Dirichlet, and Sommerfeld cases.

In addition to the situation in which the boundary is aligned with a coordinate surface, we examine the presence of corners in the computational domain. We find that, at a corner, there are compatibility conditions which the boundary data and its derivatives must satisfy and that, in general, achieving consistency of a finite difference scheme can be troublesome. We present several numerical experiments aimed at establishing or confirming the well-posedness or ill-posedness of a problem and the consistency of the numerical boundary conditions at the corners. In the case of a smooth boundary we are able to find stable discretizations for all three cases. However, when a corner is present no stable discretization was found for the Sommerfeld case. Finally, we propose an alternative implementation of the Sommerfeld boundary conditions that would preserve the constraints, offer a good approximation for absorbing boundary conditions, and eliminate the problem of the corners.

Chapter 1

Introduction

In 1993 Joseph Taylor and Russel Hulse won the Nobel Prize "for the discovery of a new type of pulsar, a discovery that has opened up new possibilities for the study of gravitation". By carefully measuring the orbiting period of the binary pulsar, they indirectly proved the existence of gravitational waves [1]. These ripples in the curved fabric of space-time are predicted by Einstein's general theory of relativity (1916) and are produced whenever two massive objects, such as black holes or neutron stars, orbit each other and collide.

An entirely new way of studying the Universe, especially its most dramatic events, will be offered to us by instruments capable of detecting and measuring gravitational radiation, such as the Laser Interferometer Space Antenna (LISA) and the Laser Interferometer Gravitational-Wave Observatory (LIGO), which consists of two facilities, one near Hanford, Washington, and the other near Livingston, Louisiana. Theoretical calculations have shown that the strongest gravitational waves that will reach the Earth will be produced by the coalescence of black holes and neutron stars and will alternately stretch and shrink distances by a factor of 10^{-21} (the Earth-Sun distance would change by roughly the size of an atom). Such a weak signal will be buried in the detector's noise. In order to measure it a prior knowledge of the possible kinds of signals is necessary. While the waveforms generated during the inspiral (before the coalescence) and the ringdown (after the coalescence) are well understood, the gravitational radiation generated during the merger of black holes or neutron stars is not. The only viable way to gain knowledge of these signals is to carry out numerical simulations on supercomputers.

According to General Relativity, time and space are united to form "space-time", a four dimensional manifold with a Lorentzian metric which satisfies Einstein's equations,

$$G_{\mu\nu} = 8\pi T_{\mu\nu},$$

ten coupled quasilinear equations in the ten components of the metric. One of the main goals of researchers involved in the field of numerical relativity (see [2] for a review) is to numerically compute solutions of Einstein's equations that represent the collision of two black holes for the extraction of the gravitational wave forms that the detectors need. This problem has proven to be much more challenging than expected and there are many issues which remain unsolved.

Casting Einstein's equations in a form which is suitable for numerical computations requires the introduction of a space-like foliation of space-time and their decomposition into two subsystems of equations: constraint equations that must be obeyed on each time slice, and evolution equations that describe how quantities propagate from one hypersurface to the next. With some manipulations, the evolution equations can be cast in symmetric hyperbolic form [3, 4, 5] and integrated numerically on a computer.

Most numerical simulations of dynamical black hole space-times that do not exploit any symmetries break down well before the relevant information can be extracted, for reasons that are not yet fully understood. When a numerical simulation "crashes", large constraint violations are observed. Although this is most likely the effect, rather than the cause, of large errors in the main variables of the system, considerable effort has been directed toward the creation of schemes that, in different ways, minimize the constraint growth as in, for example, [6]. Particular attention has been given to the problem of preventing constraint-violating modes from entering the computational domain through constraint-preserving boundary conditions when time-like boundaries are present, the hope being that this would prolong the life-time of current simulations.

Initial data cannot be specified arbitrarily. If they do not satisfy the initial value constraints, then some of the components of the vacuum Einstein equations will not be satisfied. An issue that has often been overlooked in the past is that a similar kind of restriction occurs at the boundaries. If the boundary data does not satisfy the constraints, or at least a subset of them, then one will not obtain a solution of the vacuum Einstein's equations. This is illustrated in Fig. 1.1.

One could argue that if the boundaries are sufficiently far away, one need not worry about this constraint violation, since the error introduced will mainly affect the region near the boundaries and the error might be small. The point is that in 3D numerical simulations involving black holes or neutron stars one cannot place the boundaries too far away, because of lack of computational resources. It is expected that, at least for another decade, no supercomputer in the world will have sufficient memory and computational power to allow the placing of boundaries at such great distances that their effect can be neglected for the desired amount of time. With today's technology, the errors introduced by an incorrect boundary treatment are not

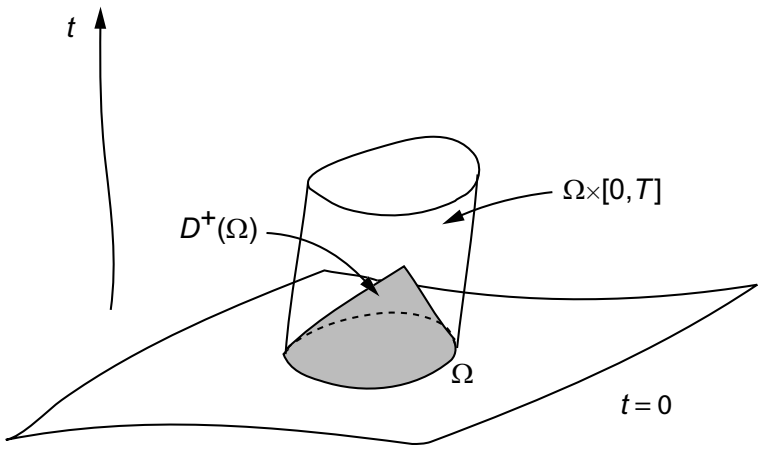

Figure 1.1: Only two of the three spatial dimensions are represented for illustrative purposes. If the constraints vanish initially in Ω, then they will vanish in $D^+(\Omega)$, the domain of dependence (shaded region) of Ω. Using constraint-preserving boundary conditions ensures that Einstein equations are satisfied inside the whole cylinder.

small and may very well be the cause of the instabilities that numerical relativists around the world are observing.

Additional complications arise when the computational domain is non-smooth, as is the case in the commonly used cubical domains. What makes these domains attractive is the fact that their implementation is relatively straightforward, as they naturally adapt to the Cartesian grids. However, they come with serious side effects. Most proofs of well-posedness are based on the smoothness assumption of the boundary and no general existence proofs for hyperbolic problems on non-smooth domains exist. Furthermore, compatibility conditions arise which cannot be ignored if one is interested in smooth solutions.

The fact that non-smooth domains appear in most multi-dimensional finite difference implementations and are commonly used in numerical relativity, makes their study significant. Fortunately, as was shown in 1995 by Olsson in a series of papers [7], it is possible to construct finite difference schemes for which stability results in the presence of corners hold. These schemes are based on operators that satisfy the summation by parts rule, similar to the integration by parts rule

$$\int_a^b \frac{du}{dx} v \, dx = - \int_a^b u \frac{dv}{dx} \, dx + (uv)|_a^b,$$

and stability is obtained by imposing boundary conditions through an orthogonal

projection operator. However, in general, constraint-preserving boundary conditions are not of the class for which Olsson's proof holds, i.e., they are not in maximally dissipative form (3.12).

In this dissertation we look at the generalized Einstein-Christoffel system linearized about Minkowski in Cartesian coordinates, given by Eqs. (4.13), (4.14), (4.17), (4.18), and (4.19). This is a problem with constant coefficients. Here the boundary data, in order to prevent constraint-violating modes from entering the domain, have to satisfy conditions that have the form of partial differential equations. These conditions can greatly affect the well-posedness of a problem and the stability of its finite difference approximation. This research was motivated primarily by the desire to find the answers to the following two questions:

1. Is it possible to discretize the initial-boundary value problem proposed by Calabrese, Pullin, Sarbach, Reula, Tiglio in reference [8] in a stable manner, particularly in the presence of corners?

2. Is it possible to discretize Sommerfeld (i.e. radiative) boundary conditions which preserve the constraints, Eqs. (5.5), (5.6), (5.7), and (5.8), in a stable way in more than one spatial dimension?

The boundary conditions proposed in [8], for which a proof of well-posedness is given, required a particular coupling between in- and outgoing modes. This coupling is likely to introduce large errors in the simulation of an isolated source due to reflections off the boundary surface. On the other hand, although there is no proof of stability, in the Sommerfeld case the reflections would be drastically reduced. The strategy followed in this dissertation consists in simplifying the problem as much as possible in order to isolate the competing sources of instabilities. We often return to the simple wave equation, where a large amount of mathematical literature is available, to understand some of the fundamental issues.

The major obstacle encountered during this research project was understanding compatibility and consistency conditions that arise when non-smooth domains are used. To our knowledge there are no examples in the current literature of a discretization that preserves the constraints and, at the same time, involves corners. In this work we will provide such a discretization. In addition, we show that constraint-preserving Sommerfeld boundary conditions are possible, at least for the case of a smooth boundary.

The work presented in this dissertation makes extensive use of the results obtained in references [8] and [9]. The dissertation is organized as follows. We begin by reviewing some of the most influential papers in the field which tackle the problem of artificial boundaries in general relativity. In chapter 3 we introduce the concepts of

strong and symmetric hyperbolicity, stress the importance of well-posedness and show how stable discretizations on rectangular grids can be obtained. The properties of the generalized Einstein-Christoffel system are discussed in chapter 4. In chapter 5 a boundary aligned with the Cartesian coordinates is introduced and the three different types of boundary conditions, the Neumann, the Dirichlet, and the Sommerfeld cases, are analyzed. The complications due to the presence of a corner in the domain are investigated in chapter 6. We conclude with chapters 7 and 8 where we summarize our results, and discuss future lines of research. Important material which, we feel, does not apply exclusively to any one chapter and which is important for the understanding of the results, is presented in the appendices.

This project is not directly linked to the numerical simulation of a binary black hole system and the extraction of gravitational waves, but it is an essential step that must be taken toward the achievement of this goal.

Chapter 2

Literature Review

The construction of constraint-preserving boundary conditions is an ongoing effort. Results with various degrees of success have been obtained by several research groups, including the one at LSU.

One of the most prominent works in this field is the article by Friedrich and Nagy, "The Initial Boundary Value Problem for Einstein's Vacuum Field Equations", Commun. Math. Phys., **201**, 619-655 (1999) [10]. Their analysis is purely analytical and is based on a tetrad formulation of Einstein's equations. They reduce the geometrical initial boundary value problem for Einstein's equations to an initial boundary value problem for a hyperbolic system to which the general result on maximally dissipative boundary conditions apply. They discuss the issue of controlling the conservation of the constraints. They also analyze the compatibility conditions between the initial and boundary data.

The same year Stewart published "The Cauchy problem and the initial boundary value problem in numerical relativity", Class. Quantum. Grav., **15**, 2865-2889 (1998) [11]. He emphasizes the importance of well-posedness for the problem to be numerically tractable and tries to draw attention to the available literature on partial differential equations and numerical analysis. He starts by studying the Cauchy problem and concludes that a problem is numerically tractable if it is well-posed, which is true if and only if the system in strongly hyperbolic. Stewart also observes that the constraint evolution equations have to be well-posed. In the presence of boundaries, he points out, the data has to be given to the incoming variables and he verifies that the boundary conditions satisfy the uniform Kreiss condition. As an example he discusses the Frittelli-Reula [12] formulation with unit lapse and zero shift, linearized about flat space-time. Stewart concludes that, for such system, strong well-posedness is obtained if and only if the momentum constraints are imposed on the boundary. He includes no numerical experiments.

In Calabrese, Lehner, Tiglio, "Constraint-preserving boundary conditions in numerical relativity", Phys. Rev. D, **65**, 104031 (2002) [13] the importance of boundary conditions which are consistent with the constraints is stressed, particularly for long term evolutions. The authors consider spherically symmetric black hole space-times in vacuum or with a minimally coupled scalar field, within the Einstein-Christoffel symmetric hyperbolic formulation of Einstein's equations. They analyze the characteristic propagation of the main variables and constraints. After imposing the incoming constraint at the boundary, they are left with two free modes, one of them being associated with the scalar field. A numerical scheme is constructed and numerical experiments are done to show stability and second order accuracy. It is claimed that the procedure can be implemented in a straightforward manner within any hyperbolic formulation of gravity in three dimensions. Soon after this work it became clear that, although it is certainly true that consistent boundary conditions can be easily formulated in more than one dimension, well-posedness may be hard to obtain.

Most of this dissertation is based on the work of Calabrese, Pullin, Reula, Sarbach, and Tiglio, "Well Posed Constraint-Preserving Boundary Conditions for the Linearized Einstein Equations", Commun. Math. Phys., **240**, 377-395, (2003) [8]. In this work the issue of specifying boundary conditions for the generalized Einstein-Christoffel formulation of Einstein's equations linearized around Minkowski is addressed. The fundamental idea is that by taking appropriate linear combinations of ingoing and outgoing characteristic variables it is possible to construct a closed symmetric hyperbolic system that lives on the boundary, which includes the evolution of some zero speed variables. By closing the system one can separate the boundary problem from the one at the interior. One can, in principle, solve the well-posed problem at the boundary and, from this, extract the boundary data needed for the evolution of the system at the interior. This procedure, unfortunately, does not seems to be extendible to more general scenarios, such as linearizations around a Schwarzschild black hole. Furthermore, a closed system at the boundary can be obtained only in the Neumann and Dirichlet cases.

In the paper by Szilágyi and Winicour, "Well-posed initial-boundary evolution in general relativity", Phys. Rev. D, **68**, 041501(R) (2003) [14], the authors address the issue of formulating a well-posed initial-boundary value problem for Einstein's field equations in harmonic coordinates using maximally dissipative boundary conditions. The authors are able to show that the problem is well posed for homogeneous boundary data and for data that is small in a linearized sense. They also briefly discuss the numerical implementation of such a problem with and without Cauchy-characteristic matching.

In Frittelli and Gómez, "Boundary conditions for hyperbolic formulations of the Einstein equations", Class. Quantum Grav., **20** 2379-2392 (2003) [15], it is claimed

that the projection of the Einstein equations along the normal to the boundary yields necessary and appropriate boundary conditions, since they contain (for a first order formulation) no derivatives normal to the boundary. This procedure is applied to the Einstein-Christoffel formulation in spherical symmetry, however no numerical experiments are included and the issue of well-posedness is mentioned but not analyzed.

The extension to $3+1$ dimensions is presented in "Einstein boundary conditions for the $3+1$ Einstein equations", Phys. Rev. D, **68**, 044014 (2003) [16], by the same authors. They calculate the boundary conditions for the Einstein-Christoffel formulation obtained by setting the projection of the Einstein tensor along the normal to zero in the case of vanishing shift. They make no use of the auxiliary system of propagation of the constraints implied by the evolution equations. Again, they do not address the issue of whether or not their boundary conditions lead to a well-posed initial-boundary value problem. Instead, they stress the fact that most of the formulations being used today are not strongly hyperbolic and therefore their boundary conditions seem to be the only viable ones. They conclude by conjecturing that such boundary conditions may extend the run time of numerical simulations.

Finally, in Calabrese and Sarbach, "Detecting ill posed boundary conditions in general relativity", J. Math. Phys., **44**, 3888-3899 (2003) [9], the well-posedness of recently proposed boundary conditions, including those of Frittelli and Gómez, is analyzed using the Laplace-Fourier technique. This technique, which can be applied to boundary conditions that are more general than the maximally dissipative ones, is capable of detecting the presence of ill-posed modes and is applied to the generalized Einstein-Christoffel system linearized around Minkowski. Interesting results obtained in this paper are the facts that the original Einstein-Christoffel system is ill posed when the ingoing constraint variables are set to zero and that strong hyperbolicity with maximal dissipative boundary conditions does not guarantee well-posedness.

Chapter 3

First Order Hyperbolic Systems

One of the greatest advantages of writing Einsteins' equations in hyperbolic form is that it allows one to benefit from the powerful mathematical machinery developed primarily in the last century. In this chapter we closely follow [17] and review the notion of hyperbolicity for first order systems of partial differential equations. Hyperbolic formulations have received a great deal of attention in numerical relativity, notably for the treatment of (artificial) time-like boundaries. Such boundaries are not determined by any geometrical or physical consideration. They are introduced to restrict the calculations to finite grids. As pointed out in [10], a thorough understanding of the analytical features of the initial-boundary value problem for Einstein's equations should be a prerequisite for successful numerical calculations near the boundary.

We discuss the energy method as a tool to prove well-posedness and mention the Laplace-Fourier technique as a powerful alternative for the constant coefficient case. We conclude the chapter by illustrating how stable discretizations can be obtained using finite difference operators satisfying the summation by parts rule [18] and Olsson's projector method to impose boundary conditions in maximally dissipative form.

3.1 Strong and Symmetric Hyperbolicity

Consider a linear, first order, system of partial differential evolution equations in three spatial dimensions,

$$\frac{\partial u}{\partial t} = \sum_{i=1}^{3} A^i \frac{\partial u}{\partial x^i}\,, \qquad (t, \vec{x}) \in [0, T] \times \Omega\,, \tag{3.1}$$

where $u = u(t, \vec{x})$ is a real vector valued function with m components, and A^i is a constant $m \times m$ real matrix. In the following, we will use the abbreviations $\partial_t = \frac{\partial}{\partial t}$,

$\partial_i = \frac{\partial}{\partial x^i}$ and Einstein's summation convention: we sum over repeated indices. With this notation, the system above can be written as $\partial_t u = A^i \partial_i u$. For the solution to be unique we need to supplement the problem with initial data

$$u(0, \vec{x}) = f(\vec{x}) \,, \qquad \vec{x} \in \Omega \,, \tag{3.2}$$

and, assuming that the boundary of Ω is non-empty, with boundary data

$$Lu(t, \vec{x}) = g(t, \vec{x}) \,, \qquad (t, \vec{x}) \in [0, T] \times \partial\Omega \,. \tag{3.3}$$

When the domain Ω is equal to $\mathbb{R}^3$, we have an initial value problem. Otherwise, its boundary is assumed to be either a $x^1 = \text{const.}$ plane or the surface of a rectangular parallelepiped $[x^1_{\min}, x^1_{\max}] \times [x^2_{\min}, x^2_{\max}] \times [x^3_{\min}, x^3_{\max}]$, and we have an initial-boundary value problem. Notice that in the last case the boundary is a non-smooth surface. The operator L and the data g that appear in the boundary condition (3.3) will be defined later.

The system (3.1) is said to be *strongly hyperbolic* if the matrix

$$\hat{P}(\vec{\omega}) = A^j \omega_j \,, \tag{3.4}$$

with $\vec{\omega} \in \mathbb{R}^3$ and $|\vec{\omega}|^2 = \omega_1^2 + \omega_2^2 + \omega_3^2 = 1$, can brought into real diagonal form by a transformation $T(\vec{\omega})$, such that $T(\vec{\omega})$ and $T^{-1}(\vec{\omega})$ are uniformly bounded with respect to $\vec{\omega}$. Moreover, the system is said to be *symmetric* hyperbolic if there exists a constant, symmetric, positive definite matrix H, independent of $\vec{\omega}$, such that

$$HA^i = (HA^i)^T \tag{3.5}$$

for $i = 1, 2, 3$. The matrix H is usually called the *symmetrizer*. If (3.5) holds for $H = 1$, then the system is said to be in explicit symmetric form. Clearly, a symmetric hyperbolic system is also strongly hyperbolic. Strong hyperbolicity is a necessary condition for well-posedness and consequently for the construction of stable numerical schemes.

The *characteristic speeds* in the direction $\vec{n} = (n_1, n_2, n_3) \in \mathbb{R}^3$, with $n_1^2 + n_2^2 + n_3^2 = 1$, are the eigenvalues of $A^n \equiv A^i n_i$. The maximum value of the characteristic speeds in the region $[0, T] \times \Omega$ can be used to compute an upper bound for the ratio between the time step and the spatial mesh size.

3.1.1 Well-posedness

The notion of a well-posed problem was first introduced by the French mathematician Jacques Hadamard in a paper published in 1902 [19]. A well-posed problem is a problem that is uniquely solvable and is such that the solution depends continuously on

the data. If the solution depended in a discontinuous way, then small errors, whether numerical errors, measurement errors, or perturbations caused by noise, could create large deviations which would lead to a loss of predictive power. The numerical treatment of ill-posed problems, which, contrary to what Hadamard claimed in his paper, can be physically interesting [20], is a great challenge. If given the option, however, one should certainly try to formulate the problem in a well-posed manner before proceeding with its discretization.

The specification of boundary conditions requires careful consideration as it can have a great impact on the well-posedness of a problem. Two of the most commonly used techniques to prove well-posedness for an initial-boundary value problem are the energy method and the Laplace-Fourier technique. The first method is quite flexible, in that it allows for variable coefficients and more generic domains. However, when it works, it gives only sufficient conditions for well-posedness. The Laplace-Fourier technique, on the other hand, gives necessary and sufficient conditions and it can be applied to boundary conditions that are more general. Unfortunately, the application of this technique to the non-constant coefficient case seems to be rather complicated.

3.1.1.1 The Energy Method

Using the energy method one can easily obtain well-posed boundary conditions [21, 22]. One defines the energy of the system at time t to be

$$E(t) = \|u(t,\cdot)\|_H^2 = \int_\Omega u^T(t,\vec{x}) H u(t,\vec{x})\, d^3x\,, \tag{3.6}$$

where H is some constant positive definite $m \times m$ symmetric matrix and u^T denotes the transpose of u. To ensure continuous dependence of the solution on the initial and boundary data, the energy must be bounded in terms of appropriate norms of the data. The procedure that is typically followed to determine this bound consists in taking a time derivative of (3.6), with the further assumptions that u is a smooth solution of (3.1) and that H is a symmetrizer. This gives

$$\frac{d}{dt}E(t) = \int_{\partial\Omega} u^T H A^n u\, d^2\sigma\,, \tag{3.7}$$

where Gauss' theorem was used in the right hand side and n_i is the outward unit normal to the boundary $\partial\Omega$. To control the growth of the energy of the solution, we naturally need to control the boundary integral. For the moment we assume that $\partial\Omega$ is smooth so that n_i is well defined.

The matrix HA^n, being symmetric, can be brought into diagonal form by an orthogonal transformation $Q(n)$,

$$Q^T(n)HA^nQ(n) = \Lambda = \mathrm{diag}(\Lambda_+, -\Lambda_-, 0)\,, \tag{3.8}$$

where $\Lambda_\pm > 0$ are positive definite diagonal matrices, the eigenvalues of which do not necessarily coincide with the characteristic speeds. By introducing the vector

$$w^{(n)} = (w^{(+\Lambda_+;n)}, w^{(-\Lambda_-;n)}, w^{(0;n)})^T = Q^T(n)u$$

one can rewrite the integrand of the boundary integral in Eq. (3.7) as the difference between two non-negative terms,

$$u^T HA^n u = w^{(+\Lambda_+;n)^T}\Lambda_+ w^{(+\Lambda_+;n)} - w^{(-\Lambda_-;n)^T}\Lambda_- w^{(-\Lambda_-;n)}\,. \tag{3.9}$$

The components of $w^{(n)}$ are the *characteristic variables* in the direction $\vec{n}$. In particular, the components of $w^{(+\Lambda_+;n)}$ are the *ingoing* characteristic variables, and the components of $w^{(-\Lambda_-;n)}$ are the *outgoing* characteristic variables. We see that prescribing homogeneous boundary conditions ($w^{(+\Lambda_+;n)} = Sw^{(-\Lambda_-;n)}$, with S sufficiently small, i.e., $S^T\Lambda_+ S \leq \Lambda_-$), ensures that the boundary term in (3.7) will give a non-positive contribution to the energy growth. The $S = 0$ case (no coupling) is of particular interest as it usually yields a good approximation for absorbing (Sommerfeld) boundary conditions.

Thus, for homogeneous boundary conditions we have

$$\frac{d}{dt}\|u(t,\cdot)\|_H^2 \leq 0\,, \tag{3.10}$$

which implies that

$$\|u(t,\cdot)\|_H \leq \|f\|_H. \tag{3.11}$$

Similar energy estimates can be obtained for inhomogeneous boundary conditions [21, 22], i.e.,

$$w^{(+\Lambda_+;n)} = Sw^{(-\Lambda_-;n)} + g\,, \tag{3.12}$$

where g can be specified arbitrarily, as long as it satisfies compatibility conditions with the initial data.

We note that in [23, 24] Sommerfeld boundary conditions are defined for a scalar wave equation $\partial_t^2 u = c^2\nabla^2 u$ in d spatial dimensions as

$$\lim_{\substack{r\to+\infty \\ r-ct=\mathrm{const.}}} r^{(d-1)/2}\left(\partial_r u + \frac{1}{c}\partial_t u\right) = 0\,.$$

where r is the radial coordinate. However, in this work we call Sommerfeld boundary condition any boundary condition of the form (3.12) with $S = 0$.

To illustrate the importance of energy estimates such as (3.11) consider the case with no boundaries and let $\bar{f} = f + \delta$ be the result of a "small" modification of the initial data and $\bar{u}$ the correspondent solution, i.e., $\bar{u}(0, x) = \bar{f}(x)$. Since the problem is linear, the error $\bar{u} - u$, satisfies the estimate

$$\|\bar{u} - u\|_H \leq \|\bar{f} - f\|_H = \|\delta\|_H \,,$$

which shows continuous dependence of the solution on the data. The boundary conditions (3.12), when applied to a symmetric hyperbolic system, lead to a well posed problem.

Boundary conditions of the form (3.12) are sometimes referred to as *maximally dissipative* boundary conditions [25]. In this case we see that the operator L introduced in (3.3) has the form

$$L = P^{(+)}Q^T(n) - SP^{(-)}Q^T(n) \,, \tag{3.13}$$

where $P^{(+)}(w^{(+)}, w^{(-)}, w^0)^T = (w^{(+)}, 0, 0)^T$ and $P^{(-)}(w^{(+)}, w^{(-)}, w^0)^T = (0, w^{(-)}, 0)^T$.

We note that if the system is symmetric hyperbolic but not written in explicit symmetric form, one can perform the change of dependent variables $w = H^{1/2}u$, which brings it into explicit symmetric form,

$$\partial_t w = H^{1/2} A^i H^{-1/2} \partial_i w = \tilde{A}^i \partial_i w \,. \tag{3.14}$$

After the change of variables, we can construct the energy using the standard L_2 norm

$$E = \int_\Omega w^T w \, d^3x = \int_\Omega u^T H u \, d^3x \,. \tag{3.15}$$

Let A^n be symmetrizable, but not in explicit symmetric form, and let $T(n)$ the transformation that brings A^n into diagonal form,

$$T^{-1}(n) A^n T(n) = \Lambda = \mathrm{diag}\{\Lambda_+, \Lambda_-, 0\} \,, \tag{3.16}$$

where $\pm\Lambda_\pm > 0$ is diagonal, and introduce the variables

$$v = (v_+, v_-, v_0)^T = T^{-1}(n) u \,. \tag{3.17}$$

It is sometimes easier to give data directly to these quantities, which are often also called characteristic variables. To see how control of the energy growth follows, we notice that the estimate (3.7) gives

$$\frac{d}{dt} E = \int_{\partial\Omega} u^T H A^n u \, d^2\sigma = \int_{\partial\Omega} v^T T^T(n) H T(n) \Lambda v \, d^2\sigma \,. \tag{3.18}$$

The matrix $T^T(n)HT(n)$ is positive definite and commutes with the diagonal matrix Λ,

$$T^T H T \Lambda = T^T H A^n T = T^T (A^n)^T H T = \Lambda T^T H T \,.$$

This implies that it must be in block diagonal form. We have that

$$\tilde{\Lambda} = T^T(n) H T(n) \Lambda = \mathrm{diag}\{\tilde{\Lambda}_+, -\tilde{\Lambda}_-, 0\}$$

and therefore

$$u^T H A^n u = v_+^T \tilde{\Lambda}_+ v_+ - v_-^T \tilde{\Lambda}_- v_- \,.$$

3.1.1.2 The Laplace-Fourier Technique

In the constant coefficient case there exists a more powerful technique that gives necessary and sufficient conditions for well-posedness. It also allows for more general boundary conditions than the maximally dissipative ones, such as those that often arise when trying to prevent constraint-violating modes to enter the domain. This technique has been used to obtain necessary conditions for well-posedness by detecting the presence of ill-posed modes in [9]. Assuming that the boundary is located at $x = \text{const.}$, ill-posed modes are solutions of the boundary value problem of the form

$$u(t, x, y, z) = e^{st + i(\omega_y y + \omega_z z)} \tilde{u}(x) \,,$$

where $\omega_y, \omega_z \in \mathbb{Z}$ and $s \in \mathbb{C}$ with $\mathrm{Re}(s) > 0$ and $\tilde{u} \in L^2$.

3.2 Stable Discretization on Rectangular Grids

Discretizing the spatial derivatives of the right hand side of system (3.1), but leaving time continuous, leads to a system of ordinary differential equations (ODEs) called the *semi-discrete system*. The method of discretizing only the spatial variables is called the *method of lines*. The resulting system of ODEs is then solved numerically with a standard ODE solver.

In a constant coefficient problem with no lower order terms, the energy defined by a constant symmetrizer is conserved. By this we mean that the change in energy of our system is solely due to the boundary term of (3.7), which can be controlled by using, for example, maximal dissipative boundary conditions (3.12). In particular, when homogeneous boundary conditions are used, or when no boundaries are present, the energy cannot increase.

Consider the domain $\Omega = \mathbb{R}^3$ with the grid points $\vec{x}_{ijk} = (ih_1, jh_2, kh_3)$, for $i, j, k \in \mathbb{Z}$ and introduce the following scalar product

$$(u, v)_h = h_1 h_2 h_3 \sum_{ijk} u_{ijk}^T v_{ijk} \,, \tag{3.19}$$

where u and v are vector valued grid functions such that $(u, u)_h < +\infty$ and $(v, v)_h < +\infty$. In the constant coefficient case the straightforward discretization $\partial_t u = A^i D_i u$, where u now represents a vector valued grid function, and D_i is a consistent approximation of ∂_i, conserves the discrete energy

$$E = (u, Hu)_h = h_1 h_2 h_3 \sum_{ijk} u_{ijk}^T H u_{ijk} \,, \tag{3.20}$$

if the difference operators satisfy $(v, D_i u)_h + (D_i v, u)_h = 0$. Examples of operators satisfying this property are D_0 and $D_0(1 - \frac{h^2}{6} D_+ D_-)$, which are second and fourth order accurate, respectively. Definitions and properties of finite difference operators are given in appendix A.

Let us now consider a rectangular domain $\Omega = \{(x^1, x^2, x^3) \in \mathbb{R}^3 | x^1_{\min} \leq x^1 \leq x^1_{\max}, x^2_{\min} \leq x^2 \leq x^2_{\max}, x^3_{\min} \leq x^3 \leq x^3_{\max}\}$, with the grid points $\vec{x}_{ijk} = (x^1_{\min} + ih_1, x^2_{\min} + jh_2, x^3_{\min} + kh_3)$, $i = 0, \ldots, N_1$ $j = 0, \ldots, N_2$ and $k = 0, \ldots, N_3$, and $h_s = (x^s_{\max} - x^s_{\min})/N_s$, $s = 1, 2, 3$. From the continuum analysis based on the energy method we expect that boundary data should be given to the incoming characteristic variables in the direction orthogonal to the boundary surface. We now repeat the same analysis for the semi-discrete system in order to determine appropriate boundary conditions for the computational grid. In particular, we examine the application of boundary conditions at the corner points of the grid.

We define the following one dimensional scalar product between vector valued grid functions,

$$(u, v)_{h_s} = h_s \sum_{i=0}^{N_s} u_i^T v_i \sigma_i \,, \tag{3.21}$$

where $\sigma_i = \{1/2, 1, \ldots, 1, 1/2\}$. The two and three dimensional scalar products are

$$(u, v)_{h_s h_r} = h_s h_r \sum_{j=0}^{N_r} \sum_{i=0}^{N_s} u_{ij}^T v_{ij} \sigma_i \sigma_j \,, \tag{3.22}$$

$$(u, v)_h = h_1 h_2 h_3 \sum_{i=0}^{N_1} \sum_{j=0}^{N_2} \sum_{k=0}^{N_3} u_{ijk}^T v_{ijk} \sigma_i \sigma_j \sigma_k \,. \tag{3.23}$$

In the following $D^{(i)}$ represents a finite difference operator approximating ∂_i. If we approximate ∂_1 with the second order centered difference operator $D_0^{(1)}u_{ijk} = (u_{i+1,jk} - u_{i-1,jk})/(2h_1)$ in the interior ($1 \le i \le N_1 - 1$, $0 \le j \le N_2$, $0 \le k \le N_3$) and with the first order one-sided difference operators $D_+^{(1)}u_{0jk} = (u_{1,jk} - u_{0,jk})/h_1$, $D_-^{(1)}u_{N_1jk} = (u_{N_1,jk} - u_{N_1-1,jk})/h_1$ at the $x^1 = \text{const.}$ boundary we get

$$\begin{aligned} & (u, D^{(1)}v)_h + (D^{(1)}u, v)_h \\ = \;& h_3 \sum_{k=0}^{N_3} h_2 \sum_{j=0}^{N_2} \left(h_1 \sum_{i=0}^{N_1} u_{ijk} D^{(1)} v_{ijk} \sigma_i + h_1 \sum_{i=0}^{N_1} D^{(1)} u_{ijk} v_{ijk} \sigma_i \right) \sigma_j \sigma_k \\ = \;& (u_{i..}, v_{i..})_{h_2 h_3} \big|_{i=0}^{i=N_1} . \end{aligned} \tag{3.24}$$

Similarly, if $D^{(2)} = D_0^{(2)}$ in the interior and $D^{(2)} = D_\pm^{(2)}$ at the $x^2 = \text{const.}$ boundary, we have that

$$(u, D^{(2)}v)_h + (D^{(2)}u, v)_h = (u_{.j.}, v_{.j.})_{h_1 h_3} \big|_{j=0}^{j=N_2} , \tag{3.25}$$

and if $D^{(3)} = D_0^{(3)}$ in the interior and $D^{(3)} = D_\pm^{(3)}$ at the $x^3 = \text{const.}$ boundary, we have that

$$(u, D^{(3)}v)_h + (D^{(3)}u, v)_h = (u_{..k}, v_{..k})_{h_1 h_2} \big|_{k=0}^{k=N_3} . \tag{3.26}$$

If these simple finite difference operators are used in (3.1) to approximate the spatial derivatives, the time derivative of the discrete energy

$$E = (u, Hu)_h = h_1 h_2 h_3 \sum_{ijk} u_{ijk}^T H u_{ijk} \sigma_i \sigma_j \sigma_k \tag{3.27}$$

gives

$$\frac{d}{dt}E = (u_{i..}, (HA^1u)_{i..})_{h_2h_3}\big|_{i=0}^{i=N_1} + (u_{.j.}, (HA^2u)_{.j.})_{h_1h_3}\big|_{j=0}^{j=N_2} + (u_{..k}, (HA^3u)_{..k})_{h_1h_2}\big|_{k=0}^{k=N_3} . \tag{3.28}$$

According to the discrete energy estimate above, to control the energy growth due to the boundary term, one should give data to the incoming variables in the direction $\vec{n}$ orthogonal to the boundary in maximal dissipative form, as shown in Fig. 3.1. To define the unit normal at the edges and vertices of the grid we examine the contribution to the energy estimate due to one of such points [7]. Wee see that, for example, at the gridpoint belonging to an edge, (N_1, N_2, k) with $1 \le k \le N_3 - 1$, we have

$$\frac{h_2}{2} u_{N_1N_2k}^T (HA^1u)_{N_1N_2k} + \frac{h_1}{2} u_{N_1N_2k}^T (HA^2u)_{N_1N_2k} = \frac{|h|}{2} u_{N_1N_2k}^T (HA^nu)_{N_1N_2k}, \tag{3.29}$$

where $|h| = \sqrt{h_1^2 + h_2^2}$ and $\vec{n} = (h_2, h_1, 0)/|h|$ is the unit effective normal at (N_1, N_2, k) for $k = 1, \ldots, N_3 - 1$. Similar results hold at other corner points.

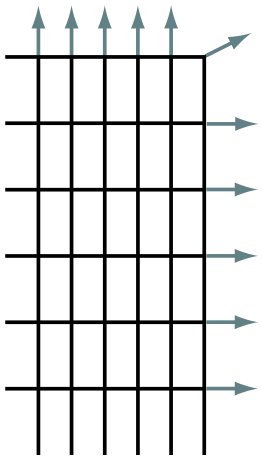

Figure 3.1: The energy estimate for the semi-discrete initial-boundary value problem on non-smooth domains shows that, in order to control the growth due to the boundary term, boundary data must be given to the incoming modes with respect to the unit normal $\vec{n}$. At the corner, the unit effective normal depends on the mesh spacings h_1 and h_2.

3.2.1 Olsson's Boundary Conditions

In [7] it is shown how to impose maximally dissipative boundary conditions at the numerical level without spoiling stability. This is done through an orthogonal projector operator P onto the subspace of gridfunctions satisfying the homogeneous boundary conditions. Let us consider a specific case. Assume that at the boundary there is one incoming, one outgoing, and one zero speed mode and that $\Lambda = \mathrm{diag}(+1, -1, 0)$, where Λ was introduced in (3.8). At each grid point belonging to the boundary, we determine the outward pointing unit normal $\vec{n} = (n_1, n_2, n_3)$ and carry out the following steps:

1. Compute $(W_{\mathrm{old}}^{(+1;n)}, W_{\mathrm{old}}^{(-1;n)}, W_{\mathrm{old}}^{(0;n)})^T = Q(n)^{-1}\Pi$, where Π is the discretized right hand side and $Q(n)$ is the orthogonal matrix that diagonalizes the boundary matrix HA^n, $Q(n)^{-1}HA^nQ(n) = \Lambda$.

2. If the boundary condition at the continuum is $w^{(+1;n)} = Sw^{(-1;n)} + g$, overwrite the ingoing and outgoing modes according to

$$W_{\mathrm{new}}^{(+1;n)} = \frac{S}{1+S^2}(SW_{\mathrm{old}}^{(+1;n)} + W_{\mathrm{old}}^{(-1;n)}) + \frac{1}{1+S^2}\partial_t g$$

$$W^{(-1;n)}_{\rm new} \;=\; \frac{1}{1+S^2}(SW^{(+1;n)}_{\rm old} + W^{(-1;n)}_{\rm old}) - \frac{S}{1+S^2}\partial_t g$$

and leave the zero speed mode unchanged, $W^{(0;n)}_{\rm new} = W^{(0;n)}_{\rm old}$. This will ensure that $W^{(+1;n)}_{\rm new} = SW^{(-1;n)}_{\rm new} + \partial_t g$ and that the following linear combination of in- and outgoing modes remains unchanged, $SW^{(+1;n)}_{\rm new} + W^{(-1;n)}_{\rm new} = SW^{(+1;n)}_{\rm old} + W^{(-1;n)}_{\rm old}$. Note that unless $S = 0$, the outgoing mode will be modified. When the exact solution is known, the boundary data required to reproduce it are $g = g^{(+1,n)} - Sg^{(-1;n)}$, where $g^{(+1;n)}$ and $g^{(-1;n)}$ are ingoing and outgoing characteristic variables of the exact solution.

3. The new modified right hand side is obtained by multiplying the new vector $(W^{(+1;n)}_{\rm new}, W^{(-1;n)}_{\rm new}, W^{(0;n)}_{\rm new})^T$ by $Q(n)$.

Alternatively, one can use $T(n)$, the transformation that brings A^n into diagonal form, in place of $Q(n)$.

Strictly speaking, the proof of stability given in [7] holds only for analytic boundary data, an assumption which does not hold for most of the experiments of the next chapters. Energy estimates for the inhomogeneous case are discussed in appendix C.

Furthermore, one should also be aware of the fact that constraint-preserving boundary conditions are usually not in maximally dissipative form.

Chapter 4

The Generalized Einstein-Christoffel System

In this chapter we introduce the generalized Einstein-Christoffel (GEC) system, as defined in subsection II.J of the article by Kidder, Scheel, and Teukolsky [4]. This is a two-parameter family of first order symmetric hyperbolic formulations of Einstein's equations. This family, or a subset of it, has been used a number of times in the recent past, particularly to derive and analyze boundary conditions which are meant to preserve the constraints. See, for example, [8, 9, 13, 15, 16].

Following [4], we outline the derivation of the GEC formulation, starting from the standard $3+1$ ADM splitting of Einstein's equation. We then specialize to the weak field regime, i.e., we consider the linearization about a Minkowski background as in [8, 9]. We briefly review the main properties of the evolution equations, the constraints, and the evolution of the constraints, the latter playing a fundamental role in the determination of constraint-preserving boundary conditions.

4.1 Casting Einstein's Equations in First Order Hyperbolic Form

According to general relativity [26], space-time is a manifold on which there is defined a Lorentz metric, ${}^{(4)}g_{\mu\nu}$, and its curvature is related to matter distribution by Einstein's equations

$$ {}^{(4)}R_{\mu\nu} - \frac{1}{2}{}^{(4)}g_{\mu\nu}{}^{(4)}R = 8\pi T_{\mu\nu}\,, \tag{4.1} $$

where ${}^{(4)}R_{\mu\nu}$ and ${}^{(4)}R$ are the Ricci tensor and the Ricci scalar associated with ${}^{(4)}g_{\mu\nu}$, and $T_{\mu\nu}$ is the stress-energy tensor. In this work we only consider the vacuum case,

i.e., from now on we assume that $T_{\mu\nu} = 0$.

If we adopt a coordinate system $\{t, x^i\}$ such that the $t =$ const. hypersurfaces are space-like and denote by n^μ the unit normal to these hypersurfaces, $n^\mu n_\mu = -1$, then the Riemannian 3-metric induced on each surface is given by

$$g_{\mu\nu} = {}^{(4)}g_{\mu\nu} + n_\mu n_\nu \,. \tag{4.2}$$

The contravariant vector field ∂_t, which is tangent to the curves with constant spatial coordinates, can be decomposed along the normal to the $t =$ const. hypersurface according to

$$\partial_t = \alpha n + \beta \,,$$

where α is the lapse function and $\beta = \beta^\mu \partial_\mu$ is the shift vector. The proper time measured by an observer traveling along n from a $t = t_0$ to a $t = t_0 + \delta t$ slice is given by $\alpha \delta t$. A translation in the direction $\beta \delta t$ will bring the observer back to a point with the same spatial coordinates it had at $t = t_0$. The line elements can be written as

$$ds^2 = -\alpha^2 dt^2 + g_{ij}(dx^i + \beta^i dt)(dx^j + \beta^j dt) \,. \tag{4.3}$$

The $3 + 1$ ADM decomposition of Einstein's equations [27, 28], used for writing these equations as an initial value problem, is obtained by projecting (4.1) along the normal to the $t =$ const. hypersurfaces. The normal components give the Hamiltonian constraint

$$\mathcal{C} \equiv \frac{1}{2}(R - K_{ij}K^{ij} + K^2) = 0 \,, \tag{4.4}$$

and the momentum constraint

$$\mathcal{C}_i \equiv \nabla_j K_i{}^j - \nabla_i K = 0 \,, \tag{4.5}$$

where ∇_i and R are the covariant derivative and scalar curvature associated with the spatial 3-metric and where K_{ij} is the extrinsic curvature of the spatial surface,

$$K_{ij} = -\frac{1}{2}\mathcal{L}_n g_{ij} \,, \tag{4.6}$$

defined in terms of the Lie derivative of the 3-metric, and $K = g^{ij}K_{ij}$. Intuitively, the extrinsic curvature corresponds to the bending of the time slice in the spacetime. Finally, the spatial components of $R_{\mu\nu} = 0$ give

$$(\partial_t - \mathcal{L}_\beta)K_{ij} = -\nabla_i \nabla_j \alpha + \alpha(R_{ij} - 2K_{il}K_j{}^l + KK_{ij}) \,, \tag{4.7}$$

where R_{ij} denotes the Ricci tensor of the 3-metric. Equations (4.6) and (4.7) are called *evolution equations*.

Although the evolution equations contain only first time derivatives, second spatial derivatives appear in (4.4) and the right hand side of (4.7). It is convenient to reduce the system to a first order one, both in space and time, so that mathematical theorems regarding the well-posedness of the problem can be more easily applied. To eliminate the second spatial derivatives from (4.4)–(4.7), one can introduce the auxiliary variables

$$d_{kij} \equiv \partial_k g_{ij} \,. \tag{4.8}$$

These variables also satisfy an evolution equation, obtained by taking a time derivative of (4.8) and using (4.6). For a solution $(g_{ij}, K_{ij}, d_{kij})$ of the evolution equations to be a solution of Einstein's equations one has to ensure that the new constraints

$$\mathcal{C}_{kij} \equiv d_{kij} - \partial_k g_{ij} \tag{4.9}$$

vanish.

Interestingly enough, the resulting system of evolution equations is only weakly hyperbolic, unless the lapse is densitized or some live gauge condition (see, for instance, [29] and references therein) is used and the constraints are judiciously added to the right hand side of the evolution equations. The lapse is densitized by introducing the lapse density Q, which is related to α and $g = \det(g_{ij})$ via

$$Q = \ln(\alpha g^{-\sigma}) \,, \tag{4.10}$$

where σ is a parameter. The lapse density and the shift vector are arbitrary functions which do not depend on the dynamical fields. They are considered source terms.

By introducing appropriate linear combinations of K_{ij} and d_{kij}, which we call P_{ij} and f_{kij}, it is possible to require that the evolution equations have a simple wave-like form. This yields a two-parameter family, called the generalized Einstein-Christoffel system. Its principal part is

$$\partial_t P_{ij} : \qquad \beta^l \partial_l P_{ij} - \alpha g^{lm} \partial_l f_{mij} \,, \tag{4.11}$$

$$\partial_t f_{kij} : \qquad \beta^l \partial_l f_{kij} - \alpha \partial_k P_{ij} \,. \tag{4.12}$$

In the next sections we fix one of the parameters and linearize these equations and the constraints about a Minkowski background in Cartesian coordinates.

4.2 The Evolution Equations

The generalized Einstein-Christoffel vacuum equations have the attractive feature that when linearized around flat space-time written in Minkowski coordinates they

simply reduce to a set of six wave equations, written in first order form:

$$\partial_t K_{ij} = -\partial^k f_{kij} \,, \tag{4.13}$$

$$\partial_t f_{kij} = -\partial_k K_{ij} \,. \tag{4.14}$$

Here, K_{ij} denotes the linearized extrinsic curvature and the symbols f_{kij} represent linear combinations of the auxiliary variables d_{kij},

$$f_{kij} = \frac{1}{2} d_{kij} + \frac{\eta - 4}{4\eta} \delta_{ij} (d_k - b_k) + \delta_{k(i} (d_{j)} - b_{j)}) \,, \tag{4.15}$$

where $d_k = d_{kij}\delta^{ij}$ and $b_j = d_{kij}\delta^{ki}$. In terms of the linearized Christoffel symbols Γ_{kij}, we have

$$f_{kij} = \Gamma_{(ij)k} + \delta^{rs} \left(\delta_{ki} \Gamma_{[sj]r} + \delta_{kj} \Gamma_{[si]r} + \frac{\eta - 4}{2\eta} \, \delta_{ij} \Gamma_{[sk]r} \right) . \tag{4.16}$$

The shift is set to zero, and the lapse is linearized in such a way that it satisfies the densitized lapse gauge condition $\alpha = \sqrt{g}$ up to second order corrections. The value of η (which must differ from zero for f_{kij} to be well defined) parametrizes the family of formulations. The particular case of $\eta = 4$ corresponds to the original Einstein-Christoffel system derived by Anderson and York [30].

4.3 The Constraints

A solution of (4.13), (4.14) is a solution of the linearized Einstein's equations if and only if the constraints are satisfied. The linearized constraint variables are

$$C \equiv \frac{\eta}{4} \, \delta^{rs} \partial_r f_s \,, \tag{4.17}$$

$$C_j \equiv \delta^{rs} \left(\partial_r K_{sj} - \partial_j K_{rs} \right) , \tag{4.18}$$

$$C_{lkij} \equiv 2\partial_{[l} f_{k]ij} + \eta \, \partial_{[l} \delta_{k](i} f_{j)} + \frac{\eta - 4}{4} \, \delta_{ij} \partial_{[l} f_{k]} \,, \tag{4.19}$$

where $f_k = \delta^{ij}(f_{kij} - f_{ijk})$. The constraints are said to be satisfied if $C = 0$, $C_j = 0$, and $C_{lkij} = 0$.

We note that the generalized Einstein-Christoffel system is similar, but not equivalent to 6 independent second order wave equations written in first order form in the following sense. When the second order wave equation $\partial_t^2 \phi = \partial^k \partial_k \phi$ is written in first order form by introducing the auxiliary variables $K = -\partial_t \phi$ and $f_k = \partial_k \phi$, the constraints $C_{lk} \equiv \partial_{[l} f_{k]} = 0$ arise. By looking at the four index constraints (4.19) it is clear that a solution of the GEC system does not necessarily satisfy $\partial_{[l} f_{k]ij} = 0$. The C_{lkij} constraints mix different ij components.

4.3.1 Evolution of the Constraint Variables

The evolution of the constraint variables plays a crucial role in the derivation of constraint-preserving boundary conditions, as it allows one to identify the ingoing and outgoing characteristic constraints at the boundary. To compute it, we follow the analysis in Refs. [8] and [9]. One assumes that the main variables satisfy the evolution equations (4.13), (4.14), takes a time derivative of the constraint variables and rewrites the right hand side in terms of the constraint variables. One can show [8] that the traceless part of C_{lkij} is constant in time, while the remaining constraints propagate according to

$$\partial_t C = \frac{\eta}{4}\,\partial^r C_r\,, \tag{4.20}$$

$$\partial_t C_j = \frac{4-2\eta}{\eta}\,\partial_j C - \partial^r T_{rj}\,, \tag{4.21}$$

$$\partial_t T_{ij} = -\partial_i C_j + \left(1-\frac{3\eta}{4}\right)\partial_j C_i + \frac{\eta}{4}\,\delta_{ij}\partial^r C_r\,, \tag{4.22}$$

$$\partial_t V_{ij} = \left(\frac{7\eta}{4}-3\right)\partial_{[i}C_{j]}\,, \tag{4.23}$$

where $T_{ij} = (C_{rij}{}^r + C_{ijr}{}^r)$, and $V_{ij} = C_{ijr}{}^r$. For $\eta \neq 2$ and $\eta \neq 8/3$, one can replace the 12 constraint variables C, T_{ij}, V_{ij} with C_{ij} and $\tilde{V}_{ij}$,

$$C_{ij} = T_{ij} + \frac{2\eta-4}{\eta}\,\delta_{ij}C\,, \tag{4.24}$$

$$\tilde{V}_{ij} = \left(\frac{3\eta}{4}-2\right)V_{ij} - \left(\frac{7\eta}{4}-3\right)T_{[ij]}\,. \tag{4.25}$$

In terms of these new variables the evolution of the constraints assumes a particularly simple form

$$\partial_t C_j = -\partial^r C_{rj}\,, \tag{4.26}$$

$$\partial_t C_{ij} = -\partial_i C_j + \kappa(\partial_j C_i - \delta_{ij}\partial^r C_r)\,, \tag{4.27}$$

$$\partial_t \tilde{V}_{ij} = 0\,, \tag{4.28}$$

where we have introduced $\kappa = 1 - 3\eta/4$.

To investigate the well-posedness of system (4.26)–(4.27), we introduce the 12 component column vector

$$u = (C_1, C_2, C_3, C_{11}, C_{12}, C_{13}, C_{21}, C_{22}, C_{23}, C_{31}, C_{32}, C_{33})^T.$$

We find that $\omega_j A^j$ is equal to

$$\begin{pmatrix}
0 & 0 & 0 & -\omega_1 & 0 & 0 & -\omega_2 & 0 & 0 & -\omega_3 & 0 & 0 \\
0 & 0 & 0 & 0 & -\omega_1 & 0 & 0 & -\omega_2 & 0 & 0 & -\omega_3 & 0 \\
0 & 0 & 0 & 0 & 0 & -\omega_1 & 0 & 0 & -\omega_2 & 0 & 0 & -\omega_3 \\
-\omega_1 & -\kappa\omega_2 & -\kappa\omega_3 & 0 & 0 & 0 & 0 & 0 & 0 & 0 & 0 & 0 \\
\kappa\omega_2 & -\omega_1 & 0 & 0 & 0 & 0 & 0 & 0 & 0 & 0 & 0 & 0 \\
\kappa\omega_3 & 0 & -\omega_1 & 0 & 0 & 0 & 0 & 0 & 0 & 0 & 0 & 0 \\
-\omega_2 & \kappa\omega_1 & 0 & 0 & 0 & 0 & 0 & 0 & 0 & 0 & 0 & 0 \\
-\kappa\omega_1 & -\omega_2 & -\kappa\omega_3 & 0 & 0 & 0 & 0 & 0 & 0 & 0 & 0 & 0 \\
0 & \kappa\omega_3 & -\omega_2 & 0 & 0 & 0 & 0 & 0 & 0 & 0 & 0 & 0 \\
-\omega_3 & 0 & \kappa\omega_1 & 0 & 0 & 0 & 0 & 0 & 0 & 0 & 0 & 0 \\
0 & -\omega_3 & \kappa\omega_2 & 0 & 0 & 0 & 0 & 0 & 0 & 0 & 0 & 0 \\
-\kappa\omega_1 & -\kappa\omega_2 & -\omega_3 & 0 & 0 & 0 & 0 & 0 & 0 & 0 & 0 & 0
\end{pmatrix}$$

and has eigenvalues $+1$, -1, and 0, with multiplicity 3, 3, and 6, respectively. Using, for example, the Maple symbolic algebra system, one can show that the most general symmetric matrix H that satisfies $HA^i = (HA^i)^T$ for $i = 1, 2, 3$ is

$$\begin{pmatrix}
1-\kappa^2 & 0 & 0 & 0 & 0 & 0 & 0 & 0 & 0 & 0 & 0 & 0 \\
0 & 1-\kappa^2 & 0 & 0 & 0 & 0 & 0 & 0 & 0 & 0 & 0 & 0 \\
0 & 0 & 1-\kappa^2 & 0 & 0 & 0 & 0 & 0 & 0 & 0 & 0 & 0 \\
0 & 0 & 0 & \frac{(1+\kappa)^2}{2\kappa+1} & 0 & 0 & 0 & -\frac{\kappa(1+\kappa)}{2\kappa+1} & 0 & 0 & 0 & -\frac{\kappa(1+\kappa)}{2\kappa+1} \\
0 & 0 & 0 & 0 & 1 & 0 & \kappa & 0 & 0 & 0 & 0 & 0 \\
0 & 0 & 0 & 0 & 0 & 1 & 0 & 0 & 0 & \kappa & 0 & 0 \\
0 & 0 & 0 & 0 & \kappa & 0 & 1 & 0 & 0 & 0 & 0 & 0 \\
0 & 0 & 0 & -\frac{\kappa(1+\kappa)}{2\kappa+1} & 0 & 0 & 0 & \frac{(1+\kappa)^2}{2\kappa+1} & 0 & 0 & 0 & -\frac{\kappa(1+\kappa)}{2\kappa+1} \\
0 & 0 & 0 & 0 & 0 & 0 & 0 & 0 & 1 & 0 & \kappa & 0 \\
0 & 0 & 0 & 0 & 0 & \kappa & 0 & 0 & 0 & 1 & 0 & 0 \\
0 & 0 & 0 & 0 & 0 & 0 & 0 & 0 & \kappa & 0 & 1 & 0 \\
0 & 0 & 0 & -\frac{\kappa(1+\kappa)}{2\kappa+1} & 0 & 0 & 0 & -\frac{\kappa(1+\kappa)}{2\kappa+1} & 0 & 0 & 0 & \frac{(1+\kappa)^2}{2\kappa+1}
\end{pmatrix}. \tag{4.29}$$

The system is symmetric hyperbolic if and only if the eigenvalues of (4.29),

$$(\kappa^2 - 1)/(2\kappa + 1), 1 - \kappa, 1 - \kappa^2, 1 + \kappa\,, \tag{4.30}$$

are positive. This confirms what was shown in [8], namely that the system is symmetric hyperbolic if the parameter η belongs to the open interval $(0, 2)$ or, equivalently, if the parameter κ belongs to the open interval $(-1/2, 1)$.

4.4 Characteristic Speeds and Characteristic Variables

The characteristic speeds of the main system are $+1$, -1 and 0, and do not depend on the direction n.

The characteristic variables in the direction n are

$$v_{ij}^{(+1;n)} = \frac{1}{\sqrt{2}}(K_{ij} - f_{nij}) , \tag{4.31}$$

$$v_{ij}^{(-1;n)} = \frac{1}{\sqrt{2}}(K_{ij} + f_{nij}) , \tag{4.32}$$

$$v_{Aij}^{(0;n)} = f_{Aij} , \tag{4.33}$$

where A represents the two directions orthogonal to n, i.e., $\delta^{ij} n_i A_j = 0$. These variables are used in the specification of boundary conditions. If n is the outward pointing unit vector orthogonal to the boundary, then $v_{ij}^{(+1;n)}$ and $v_{ij}^{(-1;n)}$ represent the ingoing and outgoing characteristic variables, respectively, and A is tangent to the boundary surface. When written in terms of the characteristic variables, the evolution equations have the form

$$\partial_t v_{ij}^{(\pm 1;n)} = \pm \partial_n v_{ij}^{(\pm 1;n)} - \frac{1}{\sqrt{2}} \partial_A v_{Aij}^{(0;n)} , \tag{4.34}$$

$$\partial_t v_{Aij}^{(0;n)} = -\frac{1}{\sqrt{2}} \partial_A (v_{ij}^{(+1;n)} + v_{ij}^{(-1;n)}) . \tag{4.35}$$

In terms of the characteristic variables in the direction n the primitive variables are given by the inverse transformation of (4.31)–(4.33),

$$K_{ij} = \frac{1}{\sqrt{2}}(v_{ij}^{(+1;n)} + v_{ij}^{(-1;n)}) , \tag{4.36}$$

$$f_{kij} = \frac{n_k}{\sqrt{2}}(-v_{ij}^{(+1;n)} + v_{ij}^{(-1;n)}) + A_k v_{Aij}^{(0;n)} . \tag{4.37}$$

As we saw in the previous section, the characteristic speeds of the evolution of the constraints are $+1$, -1, and 0, independent of n. The characteristic constraint variables in the direction n are

$$V_j^{(+1;n)} = \frac{1}{\sqrt{2}} (C_j - C_{nj}) , \tag{4.38}$$

$$V_j^{(-1;n)} = \frac{1}{\sqrt{2}} (C_j + C_{nj}) , \tag{4.39}$$

$$V^{(0;n)}_{Aj} = C_{Aj} + \kappa\left(\delta_{nj}C_{nA} - \delta_{Aj}C_{nn}\right), \tag{4.40}$$

$$\tilde{V}^{(0;n)}_{ij} = -\frac{7\kappa+2}{3}C_{[ij]} + (\kappa+1)V_{ij}\,, \tag{4.41}$$

where

$$C_j = \left(\partial^r K_{rj} - \partial_j K\right), \tag{4.42}$$

$$C_{ij} = \left(\partial^r f_{ijr} - \partial_j f_{ir}{}^r\right) + \kappa\partial_j f_i - \kappa\delta_{ij}\partial^r f_r\,. \tag{4.43}$$

In the next section we carry out numerical experiments with system (4.26)–(4.27), confirming that numerical stability can be obtained for essentially all values of the parameter κ.

4.5 Numerical Tests

Numerical experiments in $3+1$ dimensions tend to be time consuming and inconclusive. Most of the tests that we perform are meant to establish the well- or ill-posedness of a problem. It is of fundamental importance to be able to compare simulations done at different resolutions, including high resolution. For this reason, we make a symmetry assumption in the solution and the data of the problem that enables us to eliminate one of the spatial dimensions. We assume that the initial and boundary data is z independent. This allows us to eliminate all the ∂_z terms from the problem and to reduce it to a two dimensional one.

The evolution equations are identical to the ones obtained by reducing the second order wave equation to first order. Their numerical properties, in the absence of boundaries, are well known. If the partial derivatives are approximated using second order difference operators and the time integration is done with third or fourth order Runge-Kutta, then the Courant factor, the maximum ratio between the time step and the spatial mesh size that gives stability, is $\sqrt{3/d}$ and $\sqrt{8/d}$, respectively, where d is the dimensionality of the space. See Appendix C of [31] for more details.

In this section we report on numerical experiments done to confirm that a consistent and stable discretization of the evolution of the constraint variables is possible for essentially all values of the parameter κ.

In Fig. 4.1 the L_2 norm of the constraints $\|C\|_2 = (\sum_{ij}(C_r C^r + C_{rs}C^{rs})h_1 h_2)^{1/2}$ is monitored for about 10 crossing times for different values of η. Notice that for the particular case of $\eta = 4/3$ ($\kappa = 0$) the discrete L_2 norm is conserved. The time integrator is the classical fourth order Runge-Kutta and the Courant factor used is $\lambda = 2.0$. The domain is $\Omega = [0,1]\times[0,1]$ with 200 gridpoints in each direction.

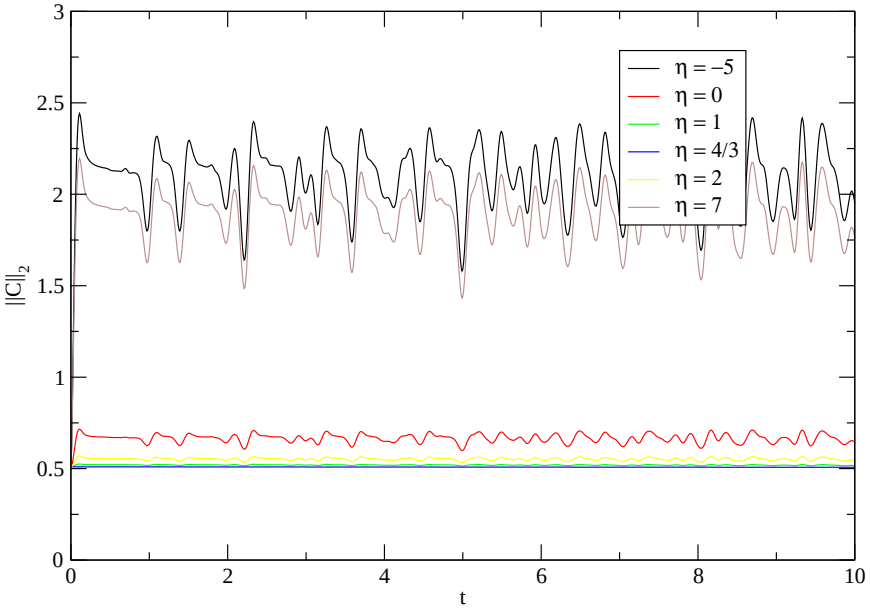

Figure 4.1: The Euclidean L_2 norm of the constraints confirms that the initial value problem for the evolution of the constraints (4.26)–(4.27) is well-posed. For $\eta = 4/3$ the norm is precisely conserved, since $H = 1$.

Chapter 5

The Half-space Problem

Chapter 4 was devoted to the study of the initial value problem for the linearized GEC system. We pointed out that, whereas the system of evolution equations for the main variables is symmetric hyperbolic for any choice of the free parameter η, the evolution of the constraint variables is symmetric hyperbolic for $\eta \in (0, 2)$ and only strongly hyperbolic otherwise. In the absence of boundaries the linearized GEC system is well posed and thus can be discretized in a stable (and consistent) way, as the numerical experiments confirm.

Now we assume that the domain is the half-space $\Omega = \{(x, y, z) \in \mathbb{R}^3 | x \geq 0\}$. As before, we want to find solutions of the evolution equations which satisfy the constraints. The half-space problem now needs, in addition to initial data, appropriate boundary data at $x = 0$ for $t \geq 0$. The issue of how to specify appropriate boundary data for the Einstein evolution equations such that (i) the constraints are preserved and (ii) the resulting initial-boundary value problem (IBVP) is well-posed is a problem of active interest in numerical relativity. Using maximal dissipative boundary conditions, Friedrich and Nagy [10] were able to find well posed constraint-preserving boundary conditions for a particular formulation of the full nonlinear vacuum equations. However, the generalized Einstein-Christoffel formulation, as most of the hyperbolic formulations used in numerical relativity, use a different set of variables than those of Ref. [10]. For these formulations the derivation of well posed constraint-preserving boundary conditions seems to be more difficult and, so far, results are limited to homogeneous boundary data or to linearization around a Minkowski background.

In addition to the two requirements above one would also like the boundary, which is a purely artificial boundary, to have as little influence as possible on the solution in the interior. By this we mean that, ideally, the solution obtained with the boundary should be the same as the one obtained with a larger domain. Unfortunately, it does

not seem to be possible to determine the boundary data that would yield the same solution at the interior without actually solving the enlarged problem or introducing some global boundary condition (see [23]).

The most commonly used technique to obtain constraint-preserving boundary conditions is based on the analysis of the evolution of the constraints. Once the incoming constraint variables are identified, one has to translate them into conditions for the incoming fields of the main system. These conditions are restrictions on the derivatives of the main variables.

Another method used in the derivation of constraint-preserving boundary conditions is the one recently proposed by Frittelli and Gómez in [15] and [16]. They obtain boundary equations from the vanishing of the projection of the Einstein tensor along the normal to the boundary surface. Although very appealing from the geometrical point of view, the well-posedness of such boundary conditions cannot be taken for granted. This issue is addressed, for example, in [9], where it is shown that the particular initial-boundary formulation proposed in [15] suffers from the presence of ill posed modes.

It is important to realize that the way boundary data is specified, i.e., the boundary conditions, can greatly affect the well-posedness of a problem. As was shown in [9], there are cases in which a well-posed initial value problem becomes an ill-posed IBVP when a boundary is introduced and a what might appear to be very innocuous boundary condition, such as setting to zero the incoming modes, is used. As we will show, the ill-posedness of certain boundary conditions that attempt to preserve the constraint can be so severe that no numerical simulation is possible.

In section 5.1 we briefly illustrate the derivation of boundary conditions that are designed to preserve the constraints based on the characteristic analysis of the evolution of the constraint variables. We focus on three different types of boundary conditions, which differ in terms of how the ingoing and outgoing fields are coupled. The three cases are:

1. Sommerfeld;
2. Neumann;
3. Dirichlet.

Whereas a proof of well-posedness is available for the Neumann and Dirichlet cases, in the Sommerfeld case only proofs of ill-posedness for certain values of the parameter η are available. Section 5.3 is devoted to the understanding of the convergence rates of the solution and its first derivatives. This is needed for the interpretation of the numerical results.

In the next chapter we will complicate the problem even further by considering the case of a non-smooth boundary, i.e., we will look at the quarter-space problem in which the domain is of the form $\Omega = \{(x, y, z) \in \mathbb{R}^3 | x \geq 0 \wedge y \geq 0\}$. We note that what is typically called quarter-space problem in the mathematical literature, such as [22] is what we have called half-space problem.

5.1 The Boundary Conditions for the GEC System

For the constraints to be satisfied everywhere, when boundaries are present, one has to ensure that no constraint-violating mode enters the domain. In order to guarantee this, we follow the analysis of Refs. [13], [8] and [9], based on the fact that, if the main variables satisfy the evolution equations, the constraint variables propagate hyperbolically. To ensure that the constraints vanish for all $t \geq 0$ one has to (i) set them to zero initially and (ii) set the incoming characteristic constraint variables to zero (or proportional to the outgoing ones). In terms of the main variables the first requirement simply means that the initial data has to satisfy the constraints. The second one means that one cannot freely specify all the incoming fields for the main system.

If n is the outward unit normal to the boundary, the ingoing and outgoing constraints are given by Eqs. (4.38) and (4.39). These equations involve normal derivatives, which cannot be controlled in hyperbolic problems. To circumvent this difficulty one typically trades the normal derivatives with time and tangential derivatives using the evolution equations. Generally, this leads to partial differential equations, which have to be satisfied by the incoming modes of the main system.

In terms of the characteristic variables for the main system, the in- and outgoing constraint variables are given by

$$V_n^{(+1;n)} = \partial_B v_{Bn}^{(+1;n)} - \partial_n v_{BB}^{(+1;n)} + \frac{\kappa}{\sqrt{2}} \partial_B f_B \,, \tag{5.1}$$

$$V_A^{(+1;n)} = \partial_n v_{nA}^{(+1;n)} + \partial_B v_{BA}^{(+1;n)} - \partial_A v_{kk}^{(+1;n)} - \frac{\kappa}{\sqrt{2}} \partial_A f_n \,, \tag{5.2}$$

$$V_n^{(-1;n)} = \partial_B v_{Bn}^{(-1;n)} - \partial_n v_{BB}^{(-1;n)} - \frac{\kappa}{\sqrt{2}} \partial_B f_B \,, \tag{5.3}$$

$$V_A^{(-1;n)} = \partial_n v_{nA}^{(-1;n)} + \partial_B v_{BA}^{(-1;n)} - \partial_A v_{kk}^{(-1;n)} + \frac{\kappa}{\sqrt{2}} \partial_A f_n \,, \tag{5.4}$$

where A and B are vectors tangent to the boundary, $f_B \equiv f_{Bkk} - f_{kkB} = v_{Bkk}^{(0;n)} - v_{AAB}^{(0;n)} + \frac{1}{\sqrt{2}}(v_{nB}^{(+1;n)} - v_{nB}^{(-1;n)})$ and $f_n \equiv f_{nBB} - f_{BBn} = -\frac{1}{\sqrt{2}}(v_{BB}^{(+1;n)} - v_{BB}^{(-1;n)}) - v_{BBn}^{(0;n)}$. We need to impose that the incoming characteristic constraint variables, $V_j^{(+1;n)}$, vanish

at the boundary either by setting them to zero or by setting them proportional to the outgoing variables, $V_j^{(-1;n)}$. In the derivation of (5.1)–(5.4) the components n_i, A_i, and B_i, are assumed to be constant.

5.1.1 Sommerfeld Case

The boundary conditions that result by setting the ingoing constraints to zero are

$$V_n^{(+1;n)} = 0: \qquad \partial_t v_{BB}^{(+1;n)} = \partial_B v_{Bn}^{(+1;n)} - \frac{1}{\sqrt{2}}\partial_A v_{ABB}^{(0;n)} + \frac{\kappa}{\sqrt{2}}\partial_B f_B\,, \tag{5.5}$$

$$V_A^{(+1;n)} = 0: \qquad \partial_t v_{nA}^{(+1;n)} = -\partial_B v_{BA}^{(+1;n)} + \partial_A v_{kk}^{(+1;n)} - \frac{1}{\sqrt{2}}\partial_B v_{BnA}^{(0;n)} + \frac{\kappa}{\sqrt{2}}\partial_A f_n\,, \tag{5.6}$$

$$v_{nn}^{(+1;n)} = g_{nn}\,, \tag{5.7}$$

$$\hat{v}_{AB}^{(+1;n)} = \hat{g}_{AB}\,, \tag{5.8}$$

where g_{nn} and $\hat{g}_{AB}$ are freely specifiable quantities, and

$$\partial_n v_{ij}^{(\pm 1;n)} = \pm\partial_t v_{ij}^{(\pm 1;n)} \pm \frac{1}{\sqrt{2}}\partial_A v_{Aij}^{(0;n)} \tag{5.9}$$

was used to trade the normal derivatives with time and tangential derivatives in (5.1) and (5.2). These boundary conditions probably represent the most natural way of obtaining constraint-preserving boundary conditions and have the great advantage that for vanishing boundary data they yield a good approximation to radiative boundary conditions. Unfortunately, to our knowledge there is currently no result showing that the resulting IBVP is well-posed. However, in [9], it was proved using the Laplace-Fourier technique that, if the parameter η lies outside the closed interval $[0, 8/3]$, the problem is ill-posed. It is interesting to notice that, in particular, the problem is ill-posed for the original Einstein-Christoffel system ($\eta = 4$).

In 2001, after having successfully carried out numerical experiments with the original Einstein-Christoffel in spherical symmetry [13], numerical tests with the three dimensional problem linearized about Minkowski clearly pointed to the fact the boundary conditions being used, Eqs. (5.5)–(5.8), were making the problem ill-posed. This stimulated the collaboration that resulted in [8], where well-posed constraint-preserving boundary conditions were obtained for two different cases, Neumann and Dirichlet.

5.1.2 Neumann Case

The idea behind the derivation of well-posed constraint-preserving boundary conditions in [8] is that, for certain couplings of in- and outgoing characteristic variables

and in- and outgoing constraints, it is possible to obtain a closed symmetric hyperbolic system that lives on the boundary. Remarkably, once some source terms are given, the boundary data can be obtained by solving this closed system without knowing anything about the solution in the interior (apart from the initial data). It is this decomposition of the problem that ensures continuous dependence on the initial and boundary data.

One of the combinations of in- and outgoing constraints that were used in [8] is

$$\frac{1}{\sqrt{2}}(V_n^{(+1;n)} + V_n^{(-1;n)}) = C_n = \partial_B K_{Bn} - \partial_n K_{BB}\,, \tag{5.10}$$

$$\frac{1}{\sqrt{2}}(V_A^{(+1;n)} - V_A^{(-1;n)}) = -C_{nA} = -\partial_n f_{nnA} - \partial_B f_{nAB} + \partial_A f_{nkk} - \kappa\partial_A f_n \tag{5.11}$$

By using the evolution equations

$$\partial_n f_{nij} = -\partial_t K_{ij} - \partial_B f_{Bij}\,, \tag{5.12}$$

$$\partial_n K_{ij} = -\partial_t f_{nij}\,, \tag{5.13}$$

we can eliminate the normal derivatives. After the trading we have

$$C_n: \quad \partial_t f_{nBB} = -\partial_B K_{Bn}\,, \tag{5.14}$$

$$C_{nA}: \quad \partial_t K_{nA} = -\partial_B f_{BnA} + \partial_B f_{nAB} - \partial_A f_{nkk} + \kappa\partial_A f_n\,. \tag{5.15}$$

In [8] it was observed that, if supplemented with the evolution of some zero speed modes, f_{ABn}, the system can be closed:

$$\partial_t f_{nBB} = -\partial_A K_{nA}\,, \tag{5.16}$$

$$\partial_t K_{nA} = -\frac{1}{2}\partial_A f_{nBB} - \partial_C f_{CAn} - \kappa\partial_A(f_{BBn} - f_{nBB}) - \partial_A f_{nnn} + \partial_B \hat{f}_{nAB}\,, \tag{5.17}$$

$$\partial_t f_{ABn} = -\partial_A K_{nB}\,. \tag{5.18}$$

Eqs. (5.16)–(5.18) form a 7×7 symmetric hyperbolic system for the variables f_{nBB}, K_{nA}, and f_{ABn}. The quantities f_{nnn} and $\hat{f}_{nAB} = f_{nAB} - \frac{1}{2}\delta_{AB} f_{nCC}$ are to be considered source terms which can be freely specified.

5.1.3 Dirichlet Case

An alternative combination of in- and outgoing constraints that was considered in [8] is

$$\frac{1}{\sqrt{2}}(V_n^{(+1;n)} - V_n^{(-1;n)}) = -C_{nn} = -\partial_B f_{nnB} + \partial_n f_{nBB} + \kappa\partial_B f_B\,, \tag{5.19}$$

$$\frac{1}{\sqrt{2}}(V_A^{(+1;n)} + V_A^{(-1;n)}) \;=\; C_A = \partial_n K_{nA} + \partial_B K_{BA} - \partial_A K_{kk}\,. \tag{5.20}$$

After the trading, one obtains the boundary conditions

$$C_{nn}: \qquad \partial_t K_{BB} = -\partial_B f_{nnB} - \partial_A f_{ABB} + \kappa \partial_B f_B\,, \tag{5.21}$$

$$C_A: \qquad \partial_t f_{nnA} = \partial_B K_{BA} - \partial_A K_{kk}\,. \tag{5.22}$$

By introducing the following combination of zero speed modes,

$$h_A = (1-\kappa) f_{ABB} + \kappa (f_{BBA} - f_{Ann})\,,$$

it is possible to construct a closed system with equations (5.21) and (5.22):

$$\partial_t K_{BB} \;=\; -(1+\kappa)\partial_A f_{nnA} - \partial_A h_A\,, \tag{5.23}$$

$$\partial_t f_{nnA} \;=\; -\frac{1}{2}\partial_A K_{BB} - \partial_A K_{nn} + \partial_B \hat{K}_{AB}\,, \tag{5.24}$$

$$\partial_t h_A \;=\; \left(\frac{\kappa}{2} - 1\right)\partial_A K_{BB} + \kappa(\partial_A K_{nn} - \partial_B \hat{K}_{BA})\,. \tag{5.25}$$

Eqs. (5.23)–(5.25) form a 5×5 symmetric hyperbolic system for the variables K_{BB}, f_{nnA}, and h_A. The quantities K_{nn} and $\hat{K}_{AB} = K_{AB} - \frac{1}{2}\delta_{AB} K_{CC}$ are to be considered source terms which can be freely specified.

5.2 Compatibility Conditions Between Initial and Boundary Data

Giving smooth initial data and smooth boundary data does not guarantee that the solution of the initial-boundary value problem is smooth. In general, there are additional conditions that the data have to satisfy.

Consider, for example, the one way wave equation

$$\partial_t u = \partial_x u \tag{5.26}$$

in $\Omega = [0,1]$ for $t \geq 0$ with initial data

$$u(0,x) = f(x)\,, \qquad 0 \leq x \leq 1\,,$$

and boundary data

$$u(t,1) = g(t)\,, \qquad t \geq 0\,.$$

Clearly, for u to be a (single-valued) function we must have that $f(1) = g(0)$. Additional requirements, called *compatibility conditions*, between the initial and boundary data arise if we demand that the solution of the problem be of class C^r.

The most general solution of the evolution equation (5.26) is given by $u(t,x) = \psi(t+x)$, where ψ is an arbitrary function. If we want u to satisfy the initial and boundary data, then we must have

$$\psi(z) = \begin{cases} f(z) & z < 1 \\ f(1) = g(0) & z = 1 \\ g(z-1) & z > 1 \end{cases} \tag{5.27}$$

The degree of smoothness of u is tied to the degree of smoothness of ψ. The function ψ is of class C^r if and only if f and g are of class C^r and

$$\lim_{x \to 1^-} \frac{d^n f}{dx^n}(x) = \lim_{t \to 0^+} \frac{d^n g}{dt^n}(t) \tag{5.28}$$

for $n = 0, 1, \ldots, r$. Condition (5.28) could have been derived by taking the n-th derivative of the boundary data, using the evolution equations n times, and taking the limit as $t \to 0^+$.

In a similar manner, one can obtain compatibility conditions for the linearized GEC system. If we look at the evolution of the constraints system we see that, for vanishing initial and boundary data, all compatibility conditions are satisfied. For the main system non trivial compatibility conditions arise for the freely specifiable data. For example, a first order compatibility condition in the Sommerfeld case is

$$[\partial_n (K_{nn} - f_{nnn}) - \partial_A f_{Ann}]_{x=0} = \sqrt{2} \partial_t g_{nn}|_{t=0} \,. \tag{5.29}$$

5.3 Convergence Rates

We emphasize that the constraints are enforced only at time $t = 0$ by restricting the set of initial data and, at the boundary, by using constraint-preserving boundary conditions. In the interior we exclusively use the evolution equations for the main variables. To test if the initial-boundary value problem can be discretized successfully one simply monitors the constraints at each time step.

Before we proceed to the testing phase of these boundary conditions, we want to gain some insight into the expected rate of convergence of the constraints in the presence of boundaries. We do so by analyzing simple toy models.

5.3.1 Initial Value Problem

We start with a case in which there are no boundaries. Consider the model problem

$$\frac{\partial u}{\partial t} = \frac{\partial u}{\partial x}\,, \qquad t \geq 0\,, \tag{5.30}$$

$$u(0,x) = f(x)\,. \tag{5.31}$$

We use the method of lines to obtain the following semi-discrete approximation

$$\frac{dv_j}{dt} = D_0 v_j\,, \qquad t \geq 0\,, \tag{5.32}$$

$$v_j(0) = f(x_j)\,. \tag{5.33}$$

To show that this is a second order accurate approximation we closely follow Ref. [22]. We need to estimate the error at time t, which is given by

$$w_j(t) = u(t,x_j) - v_j(t)\,.$$

Using (5.30) and (5.32) we see that it satisfies the equation

$$\frac{dw_j}{dt} = u_x - D_0 v_j = D_0 w_j + F_j\,, \tag{5.34}$$

where $F_j = \partial_x u(t,x_j) - D_0 u(t,x_j) = \mathcal{O}(h^2)$. The time derivative of the discrete L_2 norm of the error, $\|w\|_h^2 = \sum_j w_j^2 h$, satisfies

$$\frac{d}{dt}\|w\|_h^2 \leq 2\|w\|_h \|F\|_h\,. \tag{5.35}$$

Integrating the inequality, we get

$$\|w(t)\|_h \leq \int_0^t \|F(\tau)\|_h d\tau \approx \mathcal{O}(h^2)\,. \tag{5.36}$$

Thus, the scheme is convergent and, in particular, second order accurate. To obtain this result we relied on the fact that $F_j = \mathcal{O}(h^2)$. This condition is satisfied if the second derivative of u is Lipschitz continuous. In particular, if the exact solution is of class C^3, one has second order convergence.

We now proceed to show that the numerical derivative of v_j, $D_0 v_j$, is a second order accurate approximation to the derivative of the exact solution, $\partial_x u$. The error $w_j^{(1)}(t) = u_x(t,x_j) - D_0 v_j$ satisfies

$$\frac{dw_j^{(1)}}{dt} = u_{xx} - \frac{d}{dt} D_0 v_j = D_0 w_j^{(1)} + F_j^{(1)} \tag{5.37}$$

with $F_j^{(1)} = u_{xx}(t,x_j) - D_0 u_x(t,x_j) = \mathcal{O}(h^2)$, if $u_{xxx}(t,x)$ is Lipschitz continuous. Hence we have the inequality

$$\|w^{(1)}(t)\|_h \le \|w^{(1)}(0)\|_h + \int_0^t \|F^{(1)}(\tau)\|_h d\tau \approx \mathcal{O}(h^2)\,. \tag{5.38}$$

In this case $w^{(1)}(0)$, the initial error, is of order of the truncation error, i.e., $w^{(1)}(0) \approx \mathcal{O}(h^2)$. The above result is in agreement with [32] and can be easily generalized to show that the error in the n-th derivative, $w_j^{(n)}(t) = \partial_x^n u(t,x_j) - D_0^n v_j$, is second order accurate, provided that $\partial_x^{n+2} u$ is Lipschitz continuous.

5.3.2 Initial-boundary Value Problem

We now introduce a boundary and generalize the result of page 476 of [22]. Consider the scalar model problem

$$\frac{\partial u}{\partial t} = \frac{\partial u}{\partial x}\,, \qquad 0 \le x \le 1\,, \quad t \ge 0\,, \tag{5.39}$$

$$u(0,x) = f(x)\,, \tag{5.40}$$

$$u(t,1) = g(t)\,, \tag{5.41}$$

with real solution u. The initial and boundary data satisfy the compatibility conditions $d^n g/dt^n(0) = d^n f/dx^n(1)$ for $n = 0,1,2,\ldots,r$. The semi-discrete approximation leads to a system of ordinary differential equations

$$\frac{dv_0}{dt} = D_+ v_0\,, \tag{5.42}$$

$$\frac{dv_j}{dt} = D_0 v_j\,, \qquad j = 1,\ldots,N-1\,, \tag{5.43}$$

$$\frac{dv_N}{dt} = \frac{dg}{dt}\,, \tag{5.44}$$

$$v_j(0) = f(x_j)\,. \tag{5.45}$$

The error, $w_j(t) = u(t,x_j) - v_j(t)$, satisfies

$$\frac{dw_0}{dt} = u_x - D_+ v_0 = D_+ w_0 + F_0\,, \tag{5.46}$$

$$\frac{dw_j}{dt} = u_x - D_0 v_j = D_0 w_j + F_j \qquad j = 1,2,\ldots,N-1\,, \tag{5.47}$$

$$\frac{dw_N}{dt} = u_x - \frac{dg}{dt} = 0\,, \tag{5.48}$$

$$w(0) = 0\,, \tag{5.49}$$

where

$$F_j(t) = \begin{cases} \mathcal{O}(h), & j = 0, \\ \mathcal{O}(h^2), & j = 1, 2, \ldots, N-1 \end{cases} . \tag{5.50}$$

To estimate the order of accuracy we take a time derivative of the discrete L_2-norm of the error,

$$\begin{aligned} \frac{d}{dt}\|w(t)\|_h^2 &= 2(w, Dw)_h + 2(w, F)_h && (5.51) \\ &= -w_0^2 + w_0 F_0 h + 2(w, F)_{1,N-1} && (5.52) \\ &\leq F_0^2(t)h^2 + \|w(t)\|_h^2 + \|F(t)\|_{1,N-1}^2, && (5.53) \end{aligned}$$

and integrate the inequality (see appendix B). This gives

$$\begin{aligned} \|w(t)\|_h^2 &\leq \int_0^t e^{t-\tau} F_0^2(\tau) h^2 d\tau + \int_0^t e^{t-\tau} \|F(\tau)\|_{1,N-1}^2 d\tau && (5.54) \\ &= \mathcal{O}(h^4)\,, && (5.55) \end{aligned}$$

which proves that the approximation is second order accurate, i.e., $\|w(t)\|_h = \mathcal{O}(h^2)$.

We now want to derive a similar estimate for the discrete derivative. The error

$$\begin{aligned} w_0^{(1)}(t) &= u_x(t, x_0) - D_+ v_0\,, && (5.56) \\ w_j^{(1)}(t) &= u_x(t, x_j) - D_0 v_j\,, \qquad j = 1, \ldots, N-1\,, && (5.57) \\ w_N^{(1)}(t) &= u_x(t, x_N) - \frac{dg}{dt} = 0\,, && (5.58) \end{aligned}$$

(notice that $w_N^{(1)}(t) \neq u_x(t, x_N) - D_- v_N$) satisfies

$$\begin{aligned} \frac{dw_0^{(1)}}{dt} &= u_{xx}(t, x_0) - \frac{d}{dt} D_+ v_0 = D_+ w_0^{(1)} + F_0^{(1)}\,, && (5.59) \\ \frac{dw_j^{(1)}}{dt} &= u_{xx}(t, x_j) - \frac{d}{dt} D_0 v_j = D_0 w_j^{(1)} + F_j^{(1)}\,, \qquad j = 1, \ldots, N-1\,, && (5.60) \\ w_j^{(1)}(0) &= f_j^{(1)}\,, && (5.61) \end{aligned}$$

where

$$F_j^{(1)} = \begin{cases} \mathcal{O}(h), & j = 0, \\ \mathcal{O}(h^2), & j = 1, 2, \ldots, N-1 \end{cases} , \qquad f_j^{(1)} = \begin{cases} \mathcal{O}(h), & j = 0, \\ \mathcal{O}(h^2), & j = 1, 2, \ldots, N-1 \end{cases} . \tag{5.62}$$

Again, the initial data for the discrete derivative is not exact due to truncation errors. To obtain an estimate for $w^{(1)}(t)$ we take a time derivative of its norm

$$\begin{aligned}
\frac{d}{dt}\|w^{(1)}(t)\|_h^2 &= 2(w^{(1)}, Dw^{(1)})_h + 2(w^{(1)}, F^{(1)})_h && (5.63)\\
&= -w_0^{(1)2} + w_0^{(1)} F_0^{(1)} h + 2\sum_{j=1}^{N-1} w_j^{(1)} F_j^{(1)} h && (5.64)\\
&\leq F_0^{(1)2}(t)h^2 + \|w^{(1)}(t)\|_h^2 + \|F^{(1)}(t)\|_{1,N-1}^2 && (5.65)
\end{aligned}$$

and integrate the inequality

$$\begin{aligned}
\|w^{(1)}(t)\|_h^2 &\leq \|f^{(1)}(0)\|_h^2 + \int_0^t e^{t-\tau} F_0^{(1)2}(\tau) h^2 d\tau + \int_0^t e^{t-\tau} \|F^{(1)}(\tau)\|_{1,N-1}^2 d\tau\\
&= \mathcal{O}(h^3)\,.
\end{aligned}$$

This shows that the numerical derivative is 3/2 order accurate. Notice that the dominant contribution comes from the truncation error in the initial data at the boundary.

An important assumption in the derivation of the order of accuracy for the discretized derivative was that at the inflow boundary, $x = 1$, we defined $w_N^{(1)}$ so that it vanishes identically. However, for simplicity, when monitoring the constraints for the linearized GEC system, we will use one sided difference operators wherever a centered one cannot be used.

5.3.3 The Degree of Differentiability of the Data

It is important to know the minimum degree of smoothness of the initial and boundary data that ensures that the scheme is second order accurate.

From the analysis of this section, it follows that a sufficient condition to have second order convergence is that the solution is of class C^3. If fact, a weaker condition is that the second derivative of the exact solution is Lipschitz continuous.

Numerical experiments with a solution that has a Lipschitz continuous second derivative at a finite number of points and is smooth everywhere else indicate 3/2 order convergence for the discretized derivative.

Furthermore, to have second order convergence, it is necessary that the compatibility conditions of order 0, 1 and 2 are satisfied.

5.4 The Wave Equation

Before we proceed with the numerical experiments with the GEC system, we analyze the wave equation.

5.4.1 The Semi-discrete System and the Discrete Constraint

Consider the wave equation in two spatial dimensions,

$$\partial_t^2 \phi = \partial_x^2 \phi + \partial_y^2 \phi \,. \tag{5.66}$$

By introducing the auxiliary variables $X = \partial_x \phi$, $Y = \partial_y \phi$ and $T = \partial_t \phi$, the second order system can be written in first order symmetric hyperbolic form

$$\begin{aligned} \partial_t T &= \partial_x X + \partial_y Y \,, \\ \partial_t X &= \partial_x T \,, \\ \partial_t Y &= \partial_y T \,, \end{aligned} \tag{5.67}$$

where the constraint $C \equiv \partial_y X - \partial_x Y = 0$ has to hold. It is straightforward to see that the constraint propagates with zero speed, namely $\partial_t C = 0$. This implies that in the absence of boundaries, if the initial data satisfies the constraint, the solution at time t will satisfy the constraint. We now introduce the gridfunctions X_{ij}, Y_{ij} and T_{ij} and construct the semi-discrete system by replacing the partial derivatives with centered difference operators,

$$\begin{aligned} \partial_t T_{ij} &= D_0^{(x)} X_{ij} + D_0^{(y)} Y_{ij} \,, \\ \partial_t X_{ij} &= D_0^{(x)} T_{ij} \,, \\ \partial_t Y_{ij} &= D_0^{(y)} T_{ij} \,. \end{aligned} \tag{5.68}$$

Similarly, the discrete constraint is given by $C_{ij} = D_0^{(y)} X_{ij} - D_0^{(x)} Y_{ij}$. Since the system has constant coefficients and $[D_0^{(x)}, D_0^{(y)}] = 0$, the evolution of the discrete constraint vanishes identically,

$$\partial_t C_{ij} = [D_0^{(y)}, D_0^{(x)}] T_{ij} = 0 \,. \tag{5.69}$$

In particular, this means that if initially the discrete constraint is violated to second order in h, this will remain true during the evolution,

$$C_{ij}(t) = C_{ij}(0) = \mathcal{O}(h^2) \,,$$

and that C_{ij} will not grow in time.

5.4.2 Boundary Conditions

Let us introduce an artificial boundary at $x = 0$. We want to solve the wave equation written in first order form in the half-space $x \geq 0$. Boundary data must be provided to the incoming characteristic fields. We use the first order one sided difference operator $D_+^{(x)}$ to approximate ∂_x at the boundary. The characteristic variables in the direction $n = (-1, 0)$, the unit normal to the boundary, are

$$\begin{aligned} w^{(+1;n)} &= (T - X)/\sqrt{2}\,, & (5.70)\\ w^{(-1;n)} &= (T + X)/\sqrt{2}\,, & (5.71)\\ w^{(0;n)} &= Y\,. & (5.72) \end{aligned}$$

Following Olsson, see page 17, we overwrite the right hand side of the evolution equations at the boundary according to

$$\begin{aligned} \partial_t T_{0j} &= \frac{1}{2} D_+^{(x)} (X + T)_{0j} + \frac{1}{2} D_0^{(y)} Y_{0j} + \frac{1}{\sqrt{2}} \partial_t g_j\,,\\ \partial_t X_{0j} &= \frac{1}{2} D_+^{(x)} (X + T)_{0j} + \frac{1}{2} D_0^{(y)} Y_{0j} - \frac{1}{\sqrt{2}} \partial_t g_j\,,\\ \partial_t Y_{0j} &= D_0^{(y)} T_{0j}\,. \end{aligned} \tag{5.73}$$

Notice that the first two equations are equivalent to $\partial_t w_{0j}^{(+1;n)} = \partial_t g_j$ and $\partial_t w_{0j}^{(-1;n)} = D_+^{(x)} w_{0j}^{(-1;n)} + \frac{1}{\sqrt{2}} D_0^{(y)} w_{0j}^{(0;n)}$. In other words, while the incoming mode is overwritten by the boundary data, the outgoing mode is evolved using the evolution equations of the interior, the normal derivative being computed using a one-sided difference operator. At the boundary the constraint is discretized as

$$C_{0j} = D_0^{(y)} X_{0j} - D_+^{(x)} Y_{0j}\,. \tag{5.74}$$

If we compute its time derivative we get

$$\partial_t C_{0j} = D_0^{(y)} \left[-\frac{1}{2} D_+^{(x)} (T - X)_{0j} + \frac{1}{2} D_0^{(y)} Y_{0j} - \frac{1}{\sqrt{2}} \partial_t g_j \right]. \tag{5.75}$$

Notice that the time derivative of C_{1j}, which involves fields evaluated at the boundary, is still given by (5.69). This implies that the discretized constraint remains constant at the interior gridpoints and, in particular, it vanishes if it does so initially. Furthermore, if $D_0^{(y)} u_{ij} = 0$ at $t = 0$ and at the boundary $D_0^{(y)} g_j = 0$, then the solution satisfies $D_0^{(y)} u_{ij} = 0$ at later times. This implies that if the initial and boundary data do not depend on the y coordinate, then the constraint will vanish on the entire grid.

Assume that compatibility conditions at $t = 0$, $x = 0$ are satisfied. For $x > 0$ we have $\partial_t(T - X) = -\partial_x(T - X) + \partial_y Y$. Taking the limit $x \to 0^+$ we get

$$\partial_t g = -\frac{1}{\sqrt{2}}\partial_x(T - X) + \frac{1}{\sqrt{2}}Y_y \,. \tag{5.76}$$

This would suggest that at the boundary we have $\partial_t C_{0j} = \mathcal{O}(h)$. Therefore, we expect the convergence rate for the discretized constraint to be 3/2. We carry out a numerical experiment to confirm this.

We numerically evolve system (5.67) in $\Omega = [0, 1] \times [0, 1]$ using periodic boundary conditions in the y direction. Boundary data is given to the incoming modes at $x = 0$ and $x = 1$ according to

$$\begin{array}{rcll} w^{(+1;n)}(t, 0, y) & = & \sin^4(2\pi t)\sin^3(\pi y) & n = (-1, 0)\,, \\ w^{(+1;n)}(t, 1, y) & = & 0 & n = (+1, 0)\,, \end{array} \tag{5.77}$$

with vanishing initial data.

The contribution to the discrete constraints originates purely from the boundary. As shown in Fig. 5.1 there is a $\mathcal{O}(h)$ error at the boundary which gives a global convergence rate of 3/2. This plot was obtained using a mesh size of $h = 1/100$. The global norm is $\|C\|_h = (\sum_{ij} \sigma_i \sigma_j C_{ij}^2 h_1 h_2)^{1/2}$ and the boundary norm is its restriction to the boundary, namely, $\|C\|_h = (\sum_j \sigma_j C_{0j}^2 h_2)^{1/2}$.

5.5 Numerical Tests with the GEC System

From the work of [8] we know that both the Neumann and the Dirichlet case are well-posed provided that the parameter η belongs to the open interval $(0, 2)$. More recently, in [9], it was proved that the initial-boundary value problem for the Sommerfeld case is ill-posed if $\eta < 0$ or $\eta > 8/3$. In this section we summarize the results of numerical tests carried out to corroborate these statements and to investigate what happens in the Sommerfeld case for $0 < \eta \leq 8/3$. In the $\eta = 0$ case, the variables f_{kij} are not defined, see Eq. (4.16), and the case is therefore of no interest. To avoid corners, periodic boundary conditions in the y direction are used.

Figure 5.2 confirms the result of [9]. The parameter η is set to 2.7 and the conditions $V_j^{(+1;n)} = 0$ are used at the boundary. Time periodic data is given one of the freely specifiable incoming modes. In this specific case we choose g_{nn}.

Figure 5.3 is obtained by reducing the parameter η to 2.6. The observed stability suggests that the problem is well-posed.

Figure 5.4 summarizes the results of a parameter search for the Sommerfeld case. The test seems to confirm that for $\eta < 0$ or $\eta > 8/3$, the problem is ill posed. It

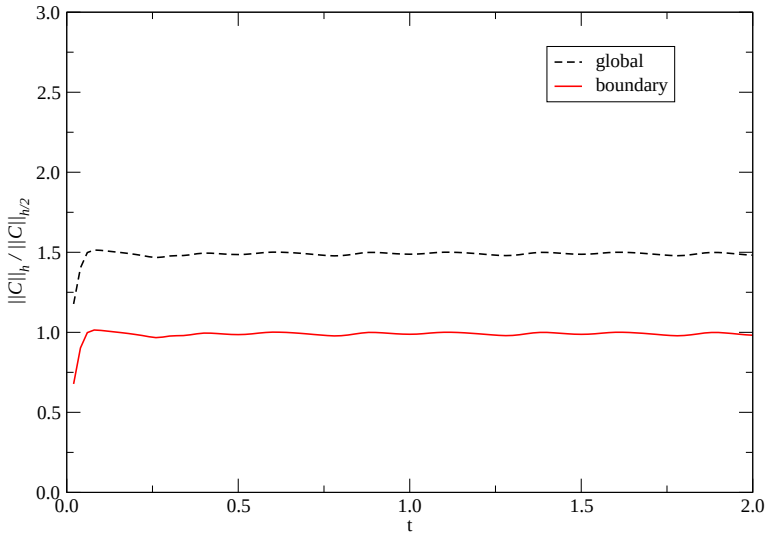

Figure 5.1: The error in the discrete constraint $C_{ij} \equiv D^{(y)}X_{ij} - D^{(x)}Y_{ij}$ is of order $\mathcal{O}(h)$ at the boundary.

is interesting to note that for sufficiently small but positive values of η the problem appears to be ill-posed, and that for values close but smaller than $8/3$ the problem appears to be well-posed. The first transition from instability to stability occurs at $\eta \approx 0.27$. It is interesting to notice that for $0 < \eta \lesssim 0.27$ both the main evolution system and the evolution of the constraint variables are symmetric hyperbolic.

We now evolve system (4.26)–(4.27) directly for $\eta = 4$ (Einstein-Christoffel system) with maximally dissipative boundary conditions $V_j^{(+1;n)} = 0$. As initial data we use a pulse of compact support which represents a "small" perturbation in the constraints. The same data of class C^3,

$$C_j = C_{ij} = \begin{cases} (1 + \cos(\pi|\vec{x} - \vec{x}_0|/r_0))^2 & |\vec{x} - \vec{x}_0| \leq r_0, \\ 0 & |\vec{x} - \vec{x}_0| > r_0 \end{cases} \tag{5.78}$$

is given to all constraint components. The results of the numerical simulations are summarized in Figure 5.5. They confirm what was shown in [9], namely that the problem is ill-posed for this particular value of the parameter. Similar plots are obtained for values of η outside the closed interval $[0, 8/3]$.

We explore the one dimensional parameter space $0 < \eta \leq 8/3$ to see if there are any values of η for which the system does not exhibit an instability. The plot in figure 5.7 suggests that setting the incoming constraints to zero leads to a well-posed

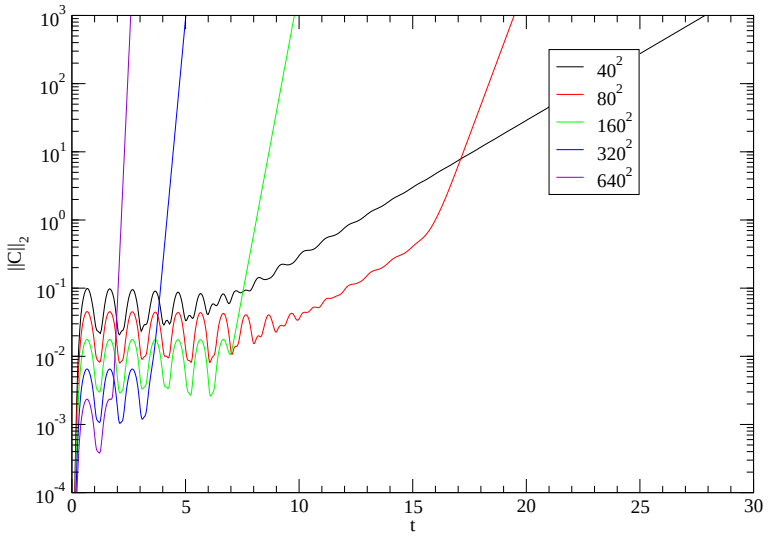

Figure 5.2: The L_2 norm of the Hamiltonian constraint at different resolutions confirms that the initial-boundary value problem for the evolution equations is ill posed for $\eta = 2.7$. As the the resolution is increased, the rate of exponential growth of the constraint increases.

problem if $0 < \eta < 8/3$. Here the instability observed in Fig. 5.4 for small but positive values of η is not present.

Tests for the $\eta = 2.6$ and $\eta = 2.7$ cases ares shown in Figs. 5.8 and 5.9.

Finally, lack of instability suggested by Fig. 5.10 confirms that, in the Neumann case, the initial-boundary value problem is well-posed. This figure was obtained with $\eta = 4/3$. Several tests done with $0 < \eta < 2$ and with the Dirichlet case also confirm stability.

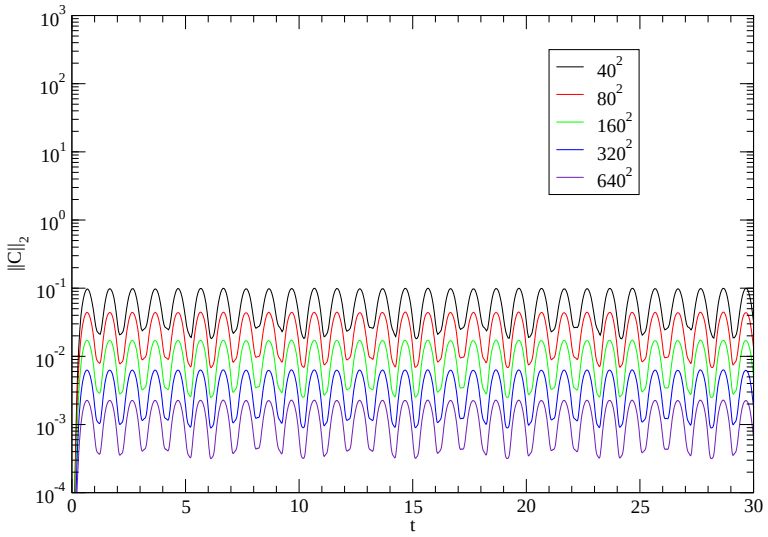

Figure 5.3: The L_2 norm of the Hamiltonian constraint for $\eta = 2.6$ in the Sommerfeld case. The constraint is converging to zero.

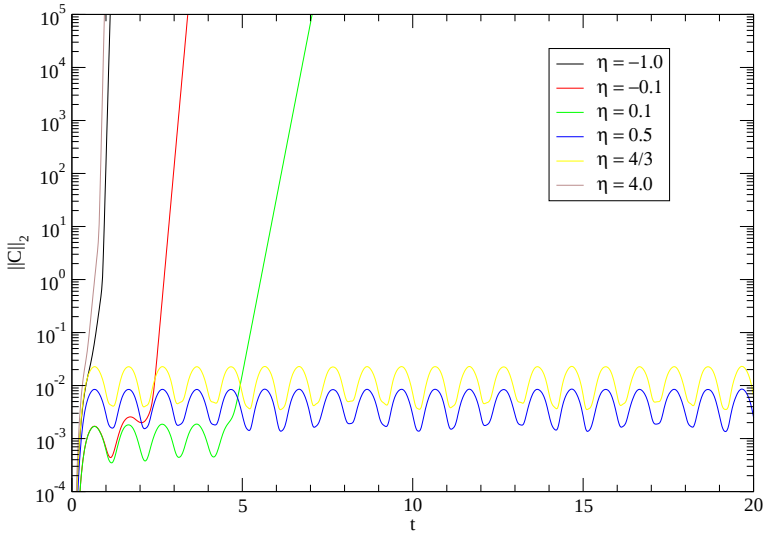

Figure 5.4: The L_2 norm of the Hamiltonian constraint for different values of the parameter η for Sommerfeld boundary conditions at a fixed resolution of 160×160.

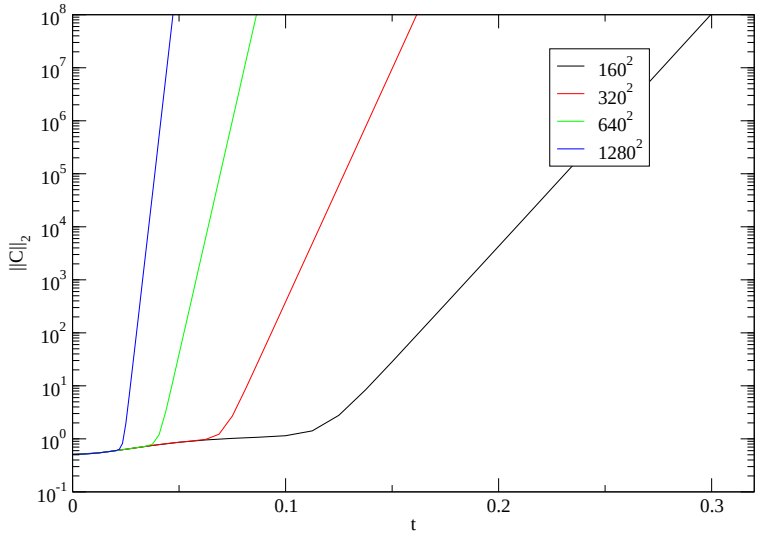

Figure 5.5: The Euclidean L_2 norm of the constraints confirms that, for $\eta = 4$, the initial-boundary value problem that results by setting the incoming constraints to zero in (4.26)–(4.27) is ill-posed. As the resolution is increased an exponentially growing mode with a frequency dependent exponent is triggered and quickly spoils the simulation. The resolutions are indicated in the legend.

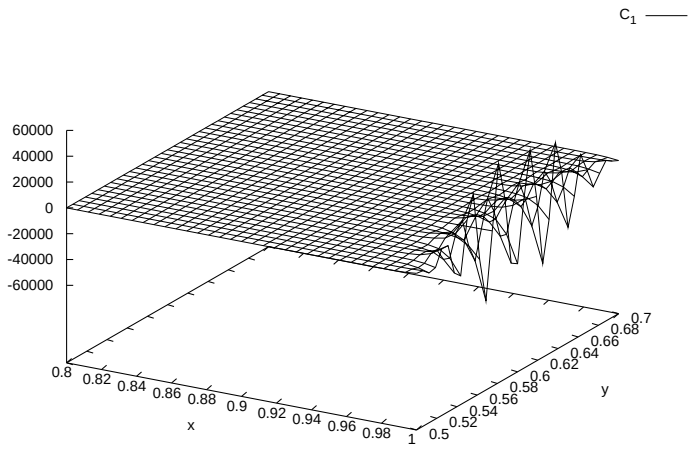

Figure 5.6: The x component of the momentum constraint, C_1, at time $t = 0.2$ for $\eta = 4$. The frequency dependent exponential growth due to the boundary conditions is evident.

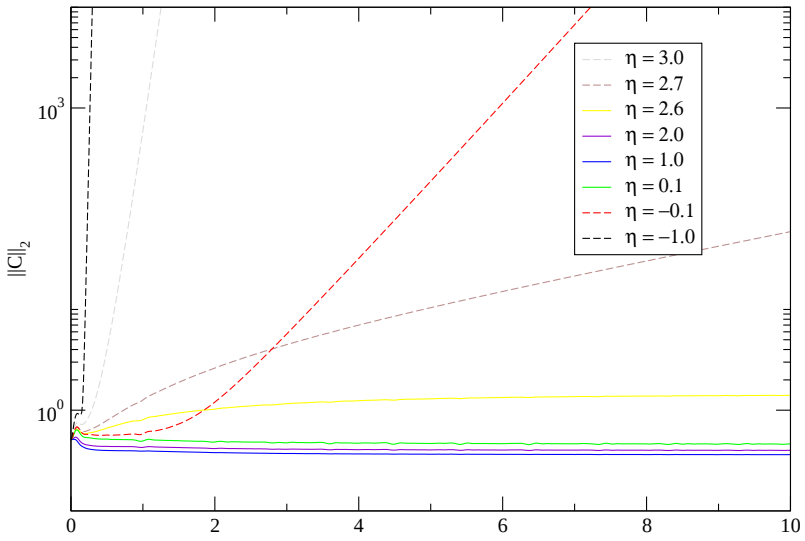

Figure 5.7: The Euclidean L_2 norm of the constraints indicates exponential growth for $\eta > 8/3$ or $\eta < 0$. The grid consists of 160×160 points.

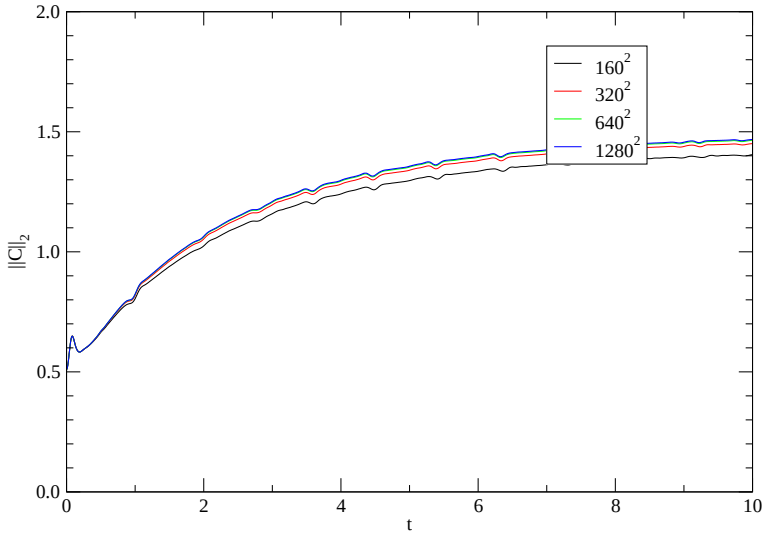

Figure 5.8: The Euclidean L_2 norm of the constraints suggests that the IBVP for the constraints is not ill-posed for $\eta = 2.6$. As the resolution is increased, the L_2 norm of the perturbation at time t seems to converge to a finite value.

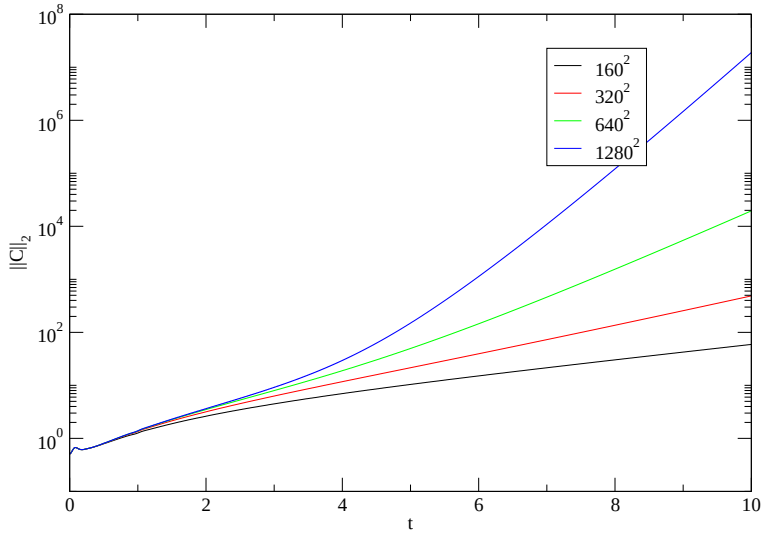

Figure 5.9: The Euclidean L_2 norm of the constraints confirms that the IBVP for the constraints is ill-posed for $\eta = 2.7$. As the resolution is increased, the L_2 norm of the perturbation increases.

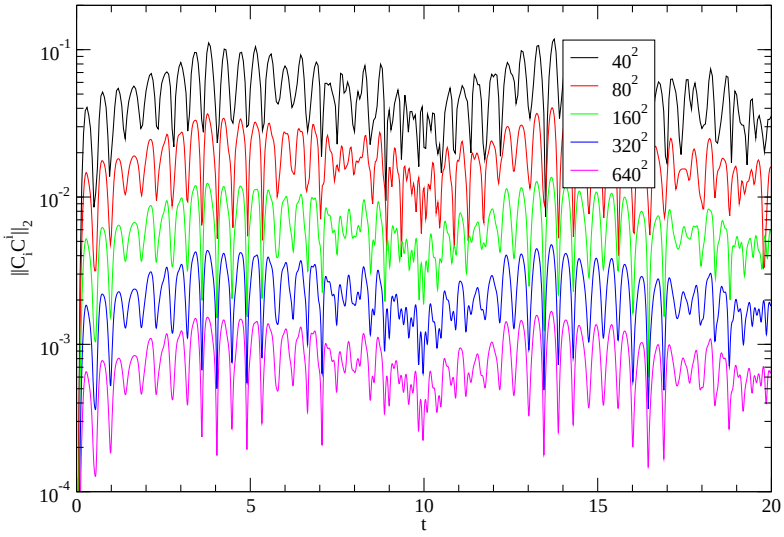

Figure 5.10: The Euclidean L_2 norm of the momentum constraints for $\eta = 4/3$ in the Neumann case suggests that the scheme is stable.

Chapter 6

The Quarter-space Problem

In this chapter we analyze boundary conditions for the initial-boundary value problem in the quarter space formed by the set of points of $\mathbb{R}^3$ with non negative x and y components,

$$\Omega = \{(x, y, z) \in \mathbb{R}^3 | x \geq 0 \wedge y \geq 0\} .$$

Its boundary, $\partial\Omega$, is clearly not smooth everywhere. There are points belonging to $\partial\Omega$ at which the unit normal is not well defined. As we will show, this gives rise to a number of complications. The fact that we would like to preserve the constraints near the corners, only makes the specification of boundary data at and in a neighborhood of such points more challenging.

Here are some of the major difficulties:

1. In order to obtain a sufficiently smooth solution, the boundary data has to satisfy *compatibility* conditions at the corners. These conditions limit the freedom with which the data can be specified and are similar to the ones that exist between the initial and boundary data.

2. At the numerical level boundary data has to be specified at the corner of the computational domain. According to Olsson's method for maximally dissipative boundary conditions data has to be given in the 45° direction for a uniform grid. Unless the exact solution is known, these boundary conditions need to be slightly modified in order to have *consistency* with the boundary data that is specified on the adjacent faces.

3. An important step in the derivation of constraint-preserving boundary conditions of the previous chapter was the use of the evolution equations to trade normal derivatives with time and tangential derivatives. The reason for doing so was that, since we are solving an hyperbolic problem, we cannot control normal

derivatives at the boundary. However, at a corner the normal unit vector is not well defined.

In section 6.1 we derive compatibility conditions for the boundary data for the two dimensional wave equation up to third order. The compatibility conditions for the generalized Einstein-Christoffel system are derived in section 6.2. We then look at the discretized wave equation and analyze the consistency of the boundary conditions at the corner. Experiments with modifications of the standard Olsson boundary conditions at the corners are summarized in section 6.4. The results of these tests clearly suggest that in order to obtain a sufficiently smooth solution, both the compatibility and consistency conditions have to be satisfied. We then test the compatibility conditions proposed in [8] and show that special attention is required in the specification of the source terms. Finally, we experiment with the Sommerfeld constraint-preserving boundary conditions in the presence of corners.

6.1 Compatibility Conditions for the Wave Equation

In this section we analyze the compatibility conditions at the corner for the two dimensional wave equation written in first order form,

$$\partial_t T = \partial_i X^i \,, \tag{6.1}$$

$$\partial_t X^i = \partial_i T \,. \tag{6.2}$$

The constraint $C \equiv \partial_{[1} X_{2]} = 0$ must hold. A compatibility condition is a relation between the derivatives of the data at two adjacent faces that must be satisfied in order to have a solution with a certain degree of smoothness. We denote with n and m the outward pointing unit vectors at the adjacent boundary faces, which meet each other at a right angle ($n \cdot m = 0$). The system has the form

$$\partial_t T = \partial_n X^n + \partial_m X^m \,, \tag{6.3}$$

$$\partial_t X^n = \partial_n T \,, \tag{6.4}$$

$$\partial_t X^m = \partial_m T \,, \tag{6.5}$$

where $\partial_n = n^i \partial_i$ and $X^n = n_i X^i$. The boundary conditions at the two sides are assumed to be in maximal dissipative form, i.e., the incoming mode is set to be equal to the sum of the outgoing mode multiplied by a sufficiently small coupling constant and an inhomogeneous term. We impose

$$T + X^n - s^{(n)}(T - X^n) = g^{(n)} \tag{6.6}$$

at the face orthogonal to n, and

$$T + X^m - s^{(m)}(T - X^m) = g^{(m)} \tag{6.7}$$

at the face orthogonal to m. A necessary condition for the problem to admit a solution of class C^r is that all of the compatibility conditions of order $j = 0, 1, \ldots, r$ are satisfied.

The procedure used to derive compatibility conditions of order r at the corner is the following. One takes time and tangential derivatives of order r of (6.6) and (6.7) and spatial derivatives of order $r - 1$ of the constraints. Using the evolution equations one eliminates the time derivatives of the main variables. One then looks for vanishing linear combinations.

- **Zeroth order**

  The only 0-th order compatibility condition is $g^{(n)} = g^{(m)}$, if $s^{(n)} = s^{(m)} = -1$. In this case we are specifying the variable T on both faces and, unless $\lim_{y\to 0^+} T(0, y, z) = \lim_{x\to 0^+} T(x, 0, z)$, the solution cannot be continuous.

- **First Order**

  A vanishing linear combination of constraints and first derivatives of boundary data is given by

$$\begin{aligned}(1 + s^{(m)})(1 + s^{(n)})C \;\; = \;\; & (1 + s^{(m)})\partial_m g^{(n)} - (1 + s^{(n)})\partial_n g^{(m)} \\ & -(1 - s^{(n)})\partial_t g^{(m)} + (1 - s^{(m)})\partial_t g^{(n)} \,,\end{aligned} \tag{6.8}$$

  where $C \equiv \partial_m X^n - \partial_n X^m$. We notice that if $s^{(n)} = -1$ or $s^{(m)} = -1$ the above compatibility condition exists even in the absence of constraints.

- **Second Order**

  We now take second time and tangential derivatives of the boundary data. In this case the compatibility condition is simply the time derivative of the first order one

$$0 = (1 + s^{(m)})\partial_t\partial_m g^{(n)} - (1 + s^{(n)})\partial_t\partial_n g^{(m)} - (1 - s^{(n)})\partial_t^2 g^{(m)} + (1 - s^{(m)})\partial_t^2 g^{(n)} \,.$$

  Furthermore, if $s_1 = s_2 = -1$ we have the additional condition

$$0 = -\partial_t^2 g^{(n)} + \partial_n^2 g^{(m)} + \partial_m^2 g^{(n)}.$$

- **Third Order**

  There are two third order compatibility conditions,

$$\begin{aligned} 0 &= (1+s^{(m)})\partial_t^2\partial_m g^{(n)} - (1+s^{(n)})\partial_t^2\partial_n g^{(m)} \\ &\quad -(1-s^{(n)})\partial_t^3 g^{(m)} + (1-s^{(m)})\partial_t^3 g^{(n)}\,, \\ (1+s^{(n)})(1+s^{(m)})(\partial_n^2-\partial_m^2)C &= (1-s^{(m)})\partial_t^3 g^{(n)} - (1-s^{(m)})\partial_t\partial_m^2 g^{(n)} \\ &\quad -(1+s^{(m)})\partial_m^3 g^{(n)} + (1+s^{(m)})\partial_t^2\partial_m g^{(n)} \\ &\quad -(1-s^{(n)})\partial_t\partial_n^2 g^{(m)} - (1+s^{(n)})\partial_n^3 g^{(m)}\,. \end{aligned}$$

6.2 Compatibility Conditions for the Linearized GEC System

In section 5.1 we showed how to obtain constraint-preserving boundary conditions for the generalized Einstein-Christoffel system linearized about Minkowski in Cartesian coordinates in the presence of a boundary aligned with the coordinates. This was done by appropriately coupling the incoming characteristic constraints to the outgoing ones. Depending on the coupling, we considered three different types of boundary conditions: Sommerfeld, Neumann, and Dirichlet. Again, we let n and m denote the unit normals to the two intersecting faces. The tangent to the edge is denoted by p. The three vectors n, m, and p, form an orthonormal basis with respect to δ_{ij}.

For convenience we rewrite these boundary conditions starting from the Sommerfeld case, in which the ingoing constraints are set directly to zero, $V_j^{(+1;n)} = 0$. Three of the incoming fields, $v_{BB}^{(+1;n)}$ and $v_{nA}^{(+1;n)}$, must satisfy a partial differential equation involving time and tangential derivatives, whereas the remaining three, $v_{nn}^{(+1;n)}$ and $\hat{v}_{AB}^{(+1;n)}$, should be freely specified,

$$\begin{aligned} v_{nn}^{(+1;n)} &= g_{nn}\,, \\ \partial_t v_{BB}^{(+1;n)} &= \partial_B v_{Bn}^{(+1;n)} - \frac{1}{\sqrt{2}}\partial_A v_{ABB}^{(0;n)} + \frac{\kappa}{\sqrt{2}}\partial_B f_B\,, \\ \partial_t v_{nA}^{(+1;n)} &= -\partial_B v_{BA}^{(+1;n)} + \partial_A v_{kk}^{(+1;n)} - \frac{1}{\sqrt{2}}\partial_B v_{BnA}^{(0;n)} + \frac{\kappa}{\sqrt{2}}\partial_A f_n\,, \\ \hat{v}_{AB}^{(+1;n)} &= \hat{g}_{AB}\,. \end{aligned}$$

We recall that the capital latin indices denote directions normal to n.

In the Neumann case the boundary conditions are

$$f_{nnn} = g_{nn}\,,$$

$$
\begin{aligned}
\partial_t f_{nBB} &= -\partial_A K_{nA}\,, \\
\partial_t K_{nA} &= -\frac{1}{2}\partial_A f_{nBB} - \partial_C f_{CAn} - \kappa\partial_A(f_{BBn} - f_{nBB}) + \partial_B \hat{f}_{nAB} - \partial_A f_{nnn}\,, \\
\hat{f}_{nAB} &= \hat{g}_{AB}\,,
\end{aligned}
$$

which ensure that $C_n = C_{nA} = 0$.

In the Dirichlet case the boundary conditions are

$$
\begin{aligned}
K_{nn} &= g_{nn}\,, \\
\partial_t K_{BB} &= -(1+\kappa)\partial_A f_{nnA} - \partial_A((1-\kappa)f_{ABB} + \kappa(f_{BBA} - f_{Ann}))\,, \\
\partial_t f_{nnA} &= -\frac{1}{2}\partial_A K_{BB} - \partial_A K_{nn} + \partial_B \hat{K}_{AB}\,, \\
\hat{K}_{AB} &= \hat{g}_{AB}\,,
\end{aligned}
$$

which guarantee that $C_{nn} = C_A = 0$.

We now assume that the same boundary conditions are used at the adjacent face with unit normal m. To obtain the first order compatibility conditions for the boundary data at an edge of the computational domain we follow the same procedure outlined in section 6.1. We momentarily neglect the fact that some boundary conditions are in differential form and assume that data is given directly to the combination

$$
(K_{ij} - f_{nij}) - s^{(n)}_{ij}(K_{ij} + f_{nij}) = \sqrt{2}(v^{(+1;n)}_{ij} - s^{(n)}_{ij} v^{(-1;n)}_{ij}) = g^{(n)}_{ij}\,,
$$

where

$$
s^{(n)}_{nn} = -s^{(n)}_{nA} = s^{(n)}_{BB} = \hat{s}^{(n)}_{AB} = \begin{cases} 0 & \text{Sommerfeld} \\ +1 & \text{Neumann} \\ -1 & \text{Dirichlet} \end{cases}\,. \tag{6.9}
$$

The data $g^{(m)}_{ij}$ and the coupling constants $s^{(m)}_{ij}$ of the adjacent face are defined in a similar manner. As before, the first order compatibility conditions at the edges are determined by taking time and tangential derivatives of the boundary data. At each face there are 6 quantities that are being specified, $g^{(n)}_{ij}$, and three possible directions (t, m and p) in which derivatives of the data can be taken. Thus, we have 18 equations on each face, giving a total of 36 equations at an edge.

By introducing the 72 component array U,

$$
U^T = (\partial_n u, \partial_m u, \partial_p u)\,,
$$

which contains all possible spatial derivatives of the 24 primitive variables $u^T =$

(K_{ij}, f_{kij}), we can write the 36 first derivatives of the boundary data in matrix form

$$\begin{pmatrix} \partial_t g^{(n)}_{ij} \\ \partial_m g^{(n)}_{ij} \\ \partial_p g^{(n)}_{ij} \\ \partial_t g^{(m)}_{ij} \\ \partial_n g^{(m)}_{ij} \\ \partial_p g^{(m)}_{ij} \end{pmatrix} = BU\,. \tag{6.10}$$

The 22 constraints, (4.17), (4.18) and (4.19), can also be written in matrix form,

$$\mathcal{C} = CU\,.$$

If the rank of the 48×72 matrix

$$L = \begin{pmatrix} B \\ C \end{pmatrix} \tag{6.11}$$

is smaller than 48, then there are first order compatibility conditions. The number of compatibility conditions is given by $48 - \mathrm{rank}(L)$.

In the remaining part of this section we summarize the results obtained in the Sommerfeld, Neumann and Dirichlet cases.

- **Sommerfeld**

  In the Sommerfeld case data is given directly to the incoming characteristic variables $K_{ij} - f_{nij} = g^{(n)}_{ij}$. We find that at the edge which is the intersection of the faces orthogonal to n and m, the following compatibility condition has to hold

  $$\tilde{C}_{nm} = +\partial_t \tilde{g}^{(n)} + \partial_m \tilde{g}^{(n)} - \partial_t \tilde{g}^{(m)} - \partial_n \tilde{g}^{(m)}\,, \tag{6.12}$$

  where

  $$\begin{aligned} \tilde{C}_{nm} &= C_{nmnn} + C_{nmmm} - 2\frac{3\eta-4}{\eta-4} C_{nmpp} && (6.13)\\ &= 2\left(\partial_{[n} f_{m]nn} + \partial_{[n} f_{m]mm} - 2\frac{3\eta-4}{\eta-4}\partial_{[n} f_{m]pp}\right)\,, \\ \tilde{g}^{(n)} &= g^{(n)}_{nn} + g^{(n)}_{mm} - 2\frac{3\eta-4}{\eta-4} g^{(n)}_{pp}\,, && (6.14)\\ \tilde{g}^{(m)} &= g^{(m)}_{nn} + g^{(m)}_{mm} - 2\frac{3\eta-4}{\eta-4} g^{(m)}_{pp}\,. && (6.15) \end{aligned}$$

This compatibility condition is an immediate consequence of the fact that the linear combinations of variables $\tilde{K} = K_{nn} + K_{mm} - 2\frac{3\eta-4}{\eta-4}K_{pp}$, $\tilde{f}_k = f_{knn} + f_{kmm} - 2\frac{3\eta-4}{\eta-4}f_{kpp}$, satisfy the first order wave equation, including the constraint $\tilde{C}_{kl} = \partial_{[k}\tilde{f}_{l]} = 0$. Condition (6.12) is simply the first order compatibility condition for the wave equation (6.8).

- **Neumann**

  At the face orthogonal to n and m data is given to a combination of in- and outgoing modes. This is summarized in Table 6.1.

Table 6.1: In the Neumann case data is given to the following quantities.

face $\perp n$	face $\perp m$
$-2f_{nnn} = g^{(n)}_{nn}$	$-2f_{mmm} = g^{(m)}_{mm}$
$+2K_{nm} = g^{(n)}_{nm}$	$+2K_{mn} = g^{(m)}_{mn}$
$+2K_{np} = g^{(n)}_{np}$	$+2K_{mp} = g^{(m)}_{mp}$
$-2f_{nmm} = g^{(n)}_{mm}$	$-2f_{mnn} = g^{(m)}_{nn}$
$-2f_{nmp} = g^{(n)}_{mp}$	$-2f_{mnp} = g^{(m)}_{np}$
$-2f_{npp} = g^{(n)}_{pp}$	$-2f_{mpp} = g^{(m)}_{pp}$

In the Neumann case there is only one zeroth order compatibility condition, $g^{(n)}_{nm} = g^{(m)}_{nm}$. This condition simply reflects the fact that since we are specifying K_{nm} on the two adjacent faces, we must ensure that as we approach the edge on both faces we give the same values. If this condition is violated, the problem cannot admit a continuous solution.

In this case we find that the rank of L in (6.11) is 41, which means that there are 7 compatibility conditions containing first derivatives of the boundary data. These are

$$
\begin{aligned}
0 &= \partial_t(g^{(n)}_{nm} - g^{(m)}_{nm})\,, && (6.16)\\
0 &= \partial_p(g^{(n)}_{nm} - g^{(m)}_{nm})\,, && (6.17)\\
0 &= \partial_t g^{(n)}_{mp} - \partial_n g^{(m)}_{mp}\,, && (6.18)\\
0 &= \partial_t g^{(m)}_{np} - \partial_m g^{(n)}_{np}\,, && (6.19)\\
2C_n &= -\partial_t g^{(n)}_{mm} - \partial_t g^{(n)}_{pp} + \partial_m g^{(n)}_{nm} + \partial_p g^{(n)}_{np}\,, && (6.20)\\
2C_m &= -\partial_t g^{(m)}_{nn} - \partial_t g^{(m)}_{pp} + \partial_n g^{(m)}_{nm} + \partial_p g^{(m)}_{mp}\,, && (6.21)
\end{aligned}
$$

$$2\tilde{C}_{nm} = \partial_m \tilde{g}^{(n)} - \partial_n \tilde{g}^{(m)} . \tag{6.22}$$

If any one of these conditions is violated, the problem cannot have a C^1 solution. Notice that the first two conditions are a trivial consequence of the zeroth order compatibility condition.

Perhaps the meaning of these conditions becomes clearer after rewriting them in terms of the primitive variables K_{ij}, f_{kij}. If we write the quantities specified on the n face on the left hand side and the quantities specified on the m face on the right hand side, the first order compatibility conditions read

$$\begin{aligned}
\partial_t K_{nm} &= \partial_t K_{nm} , && (6.23)\\
\partial_p K_{nm} &= \partial_p K_{nm} , && (6.24)\\
\partial_t f_{nmp} &= -\partial_n K_{mp} , && (6.25)\\
-\partial_m K_{np} &= \partial_t f_{mnp} , && (6.26)\\
\partial_t f_{nmm} + \partial_t f_{npp} + & && (6.27)\\
+\partial_m K_{nm} + \partial_p K_{np} &= 0 , &&\\
0 &= \partial_t f_{mnn} + \partial_t f_{mpp} + && (6.28)\\
&\quad +\partial_n K_{nm} + \partial_p K_{mp} , &&\\
\partial_m f_{nnn} + \partial_m f_{nmm} + & && (6.29)\\
-2\frac{3\eta-4}{\eta-4}\partial_m f_{npp} &= \partial_n f_{mnn} + \partial_n f_{mmm} + &&\\
&\quad -2\frac{3\eta-4}{\eta-4}\partial_n f_{mpp} . &&
\end{aligned}$$

In section (6.5) we will discuss the compatibility conditions proposed in [8] and show that, in general, the last condition (6.29) is not automatically satisfied.

- **Dirichlet**

  In the Dirichlet case boundary data is given according to Table 6.2.

  We find that there are 11 compatibility conditions:

$$\begin{aligned}
0 &= \partial_t (g^{(n)}_{nn} - g^{(m)}_{nn}) , && (6.30)\\
0 &= \partial_p (g^{(n)}_{nn} - g^{(m)}_{nn}) , && (6.31)\\
0 &= \partial_t (g^{(n)}_{mm} - g^{(m)}_{mm}) , && (6.32)\\
0 &= \partial_p (g^{(n)}_{mm} - g^{(m)}_{mm}) , && (6.33)\\
0 &= \partial_t (g^{(n)}_{pp} - g^{(m)}_{pp}) , && (6.34)
\end{aligned}$$

Table 6.2: In the Dirichlet case data is given to the following quantities.

face $\perp n$	face $\perp m$
$2K_{nn} = g^{(n)}_{nn}$	$2K_{mm} = g^{(m)}_{mm}$
$-2f_{nnm} = g^{(n)}_{nm}$	$-2f_{mmn} = g^{(m)}_{mn}$
$-2f_{nnp} = g^{(n)}_{np}$	$-2f_{mmp} = g^{(m)}_{mp}$
$2K_{mm} = g^{(n)}_{mm}$	$2K_{nn} = g^{(m)}_{nn}$
$2K_{mp} = g^{(n)}_{mp}$	$2K_{np} = g^{(m)}_{np}$
$2K_{pp} = g^{(n)}_{pp}$	$2K_{pp} = g^{(m)}_{pp}$

$$
\begin{aligned}
0 &= \partial_p(g^{(n)}_{pp} - g^{(m)}_{pp})\,, && (6.35)\\
0 &= \partial_t g^{(n)}_{np} - \partial_n g^{(m)}_{np}\,, && (6.36)\\
0 &= \partial_t g^{(m)}_{mp} - \partial_m g^{(n)}_{mp}\,, && (6.37)\\
2C_n &= \partial_t g^{(m)}_{nm} + \partial_p g^{(m)}_{np} - \partial_n g^{(m)}_{mm} - \partial_n g^{(m)}_{pp}\,, && (6.38)\\
2C_m &= \partial_t g^{(n)}_{nm} + \partial_p g^{(n)}_{mp} - \partial_m g^{(n)}_{nn} - \partial_m g^{(n)}_{pp}\,, && (6.39)\\
2C_p &= \partial_m g^{(n)}_{mp} - \partial_p g^{(n)}_{mm} + \partial_n g^{(m)}_{np} - \partial_p g^{(m)}_{nn}\,. && (6.40)
\end{aligned}
$$

The first six equations are a consequence of the zeroth order compatibility conditions $g^{(n)}_{nn} = g^{(m)}_{nn}$, $g^{(n)}_{mm} = g^{(m)}_{mm}$ and $g^{(n)}_{pp} = g^{(m)}_{pp}$.

As we did for the Neumann case, we rewrite the compatibility conditions in terms of the primitive variables

$$
\begin{aligned}
\partial_t K_{nn} &= \partial_t K_{nn}\,, && (6.41)\\
\partial_p K_{nn} &= \partial_p K_{nn}\,, && (6.42)\\
\partial_t K_{mm} &= \partial_t K_{mm}\,, && (6.43)\\
\partial_p K_{mm} &= \partial_p K_{mm}\,, && (6.44)\\
\partial_t K_{pp} &= \partial_t K_{pp}\,, && (6.45)\\
\partial_p K_{pp} &= \partial_p K_{pp}\,, && (6.46)\\
\partial_t f_{nnp} &= -\partial_n K_{np}\,, && (6.47)\\
-\partial_m K_{mp} &= \partial_t f_{mmp}\,, && (6.48)\\
0 &= \partial_t f_{mnm} - \partial_p K_{np} + && (6.49)\\
&\quad +\partial_n K_{mm} + \partial_n K_{pp}\,, &&\\
\partial_t f_{nnm} - \partial_p K_{mp} + & && (6.50)
\end{aligned}
$$

$$
\begin{aligned}
+\partial_m K_{nn} + \partial_m K_{pp} &= 0\,, \\
\partial_m K_{mp} - \partial_p K_{mm} &= -\partial_n K_{np} + \partial_p K_{nn}\,.
\end{aligned} \tag{6.51}
$$

We analyze the compatibility conditions proposed in [8] in section 6.5.

It is important to realize that, since only three of the six quantities at the boundary are freely specifiable, the remaining three being determined by differential equations, it is not obvious how to ensure that the first order compatibility conditions are satisfied during evolution.

6.3 Consistency of the Boundary Data at Corners

When dealing with a semi-discrete system approximating an initial-boundary value problem over a non-smooth domain, the additional issue of giving consistent boundary data at the corners arises.

Let us start with some simple observations. Suppose that, at a corner, data is given to the incoming mode in the direction n, $v^{(+1;n)} = g^{(n)}$, leaving the outgoing and zero speed mode unchanged. If we then overwrite the incoming mode in the m direction, $v^{(+1;m)} = g^{(m)}$, leaving the outgoing and the zero speed modes in the direction m unchanged, we no longer have that $v^{(+1;n)} = g^{(n)}$. The two operations do not commute. To see this we use a bar to denote intermediate values and write

$$
\begin{aligned}
\bar{K} - \bar{f}_n &= g^{(n)}\,, && (6.52)\\
\bar{K} + \bar{f}_n &= K^{\text{old}} + f_n^{\text{old}}\,, && (6.53)\\
\bar{f}_m &= f_m^{\text{old}}\,, && (6.54)\\
\bar{f}_p &= f_p^{\text{old}}\,, && (6.55)
\end{aligned}
$$

and

$$
\begin{aligned}
K^{\text{new}} - f_m^{\text{new}} &= g^{(m)}\,, && (6.56)\\
K^{\text{new}} + f_m^{\text{new}} &= \bar{K} + \bar{f}_m\,, && (6.57)\\
f_n^{\text{new}} &= \bar{f}_n\,, && (6.58)\\
f_p^{\text{new}} &= \bar{f}_p\,. && (6.59)
\end{aligned}
$$

The result of these two operations is

$$
K^{\text{new}} = \frac{1}{2}g^{(m)} + \frac{1}{4}g^{(n)} + \frac{1}{4}K^{\text{old}} + \frac{1}{4}f_n^{\text{old}} + \frac{1}{2}f_m^{\text{old}}\,, \tag{6.60}
$$

$$f_n^{\rm new} = -\frac{1}{2}g^{(n)} + \frac{1}{2}K^{\rm old} + \frac{1}{2}f_n^{\rm old}\,, \tag{6.61}$$

$$f_m^{\rm new} = -\frac{1}{2}g^{(m)} + \frac{1}{4}g^{(n)} + \frac{1}{4}K^{\rm old} + \frac{1}{4}f_n^{\rm old} + \frac{1}{2}f_m^{\rm old}\,, \tag{6.62}$$

$$f_p^{\rm new} = f_p^{\rm old}\,. \tag{6.63}$$

In general, as a result of the second operation, it is no longer true that

$$K^{\rm new} - f_n^{\rm new} \neq g^{(n)}\,. \tag{6.64}$$

We emphasize that even for homogeneous boundary data the operations of overwriting the data in the two directions n and m do not commute. We also note that it is not possible to simultaneously overwrite data in the n and m directions leaving the two outgoing modes unchanged. The system

$$K^{\rm new} - f_n^{\rm new} = g^{(n)}\,, \tag{6.65}$$

$$K^{\rm new} - f_m^{\rm new} = g^{(m)}\,, \tag{6.66}$$

$$K^{\rm new} + f_n^{\rm new} = K^{\rm old} + f_n^{\rm old}\,, \tag{6.67}$$

$$K^{\rm new} + f_m^{\rm new} = K^{\rm old} + f_m^{\rm old}\,, \tag{6.68}$$

is overdetermined and has no solution, unless $g^{(m)} - g^{(n)} + f_m^{\rm old} - f_n^{\rm old} = 0$.

Let us now consider the wave equation in two dimensions. The characteristic speeds and characteristic variables in the direction n, with $n_1^2 + n_2^2 = 1$ are given by

$$w^{(+1;n)} = (T + X^n)/\sqrt{2}\,, \tag{6.69}$$

$$w^{(-1;n)} = (T - X^n)/\sqrt{2}\,, \tag{6.70}$$

$$w^{(0;n)} = X^A\,, \tag{6.71}$$

where $A = n^\perp = (-n_2, n_1)$. If we introduce $w^{(n)} = (w^{(+1;n)}, w^{(-1;n)}, w^{(0;n)})^T$, $u = (T, X, Y)^T$, then the above relation can be expressed in matrix form as $w^{(n)} = Q^{-1}(n)u$, where

$$Q(n) = \begin{pmatrix} \frac{1}{\sqrt{2}} & \frac{1}{\sqrt{2}} & 0 \\ \frac{n_1}{\sqrt{2}} & -\frac{n_1}{\sqrt{2}} & n_1^\perp \\ \frac{n_2}{\sqrt{2}} & -\frac{n_2}{\sqrt{2}} & n_2^\perp \end{pmatrix} \tag{6.72}$$

is an orthogonal matrix which satisfies $Q^{-1}(n)A^nQ(n) = \mathrm{diag}(+1, -1, 0)$. The transformation between two different sets of characteristic variables is given by $w^{(t)} = Q^{-1}(t)Q(n)w^{(n)} = R(t,n)w^{(n)}$, with

$$R(t,n) = \begin{pmatrix} (1 + t\cdot n)/2 & (1 - t\cdot n)/2 & t\cdot n^\perp/\sqrt{2} \\ (1 - t\cdot n)/2 & (1 + t\cdot n)/2 & -t\cdot n^\perp/\sqrt{2} \\ -t\cdot n^\perp/\sqrt{2} & t\cdot n^\perp/\sqrt{2} & t\cdot n \end{pmatrix}. \tag{6.73}$$

Notice that $R(n,n) = 1$ and $R(n,t) = R(t,n)^{-1} = R(t,n)^T$.

Suppose that boundary data is given at the $x = 0$ and $y = 0$ face with unit normals n and m in maximal dissipative form,

$$w^{(+1;n)} = s^{(n)} w^{(-1;n)} + g^{(n)}\,, \tag{6.74}$$
$$w^{(+1;m)} = s^{(m)} w^{(-1;m)} + g^{(m)}\,. \tag{6.75}$$

We want to determine boundary conditions for the corner that satisfy (6.74) and (6.75) and give numerical stability. By giving data to the incoming fields at a 45 degree direction, one can bound the discrete energy estimate, as was shown by Olsson. The boundary conditions (6.74), (6.75), can be written as

$$(1, -s^{(n)}, 0) w^{(n)} = g^{(n)}\,, \tag{6.76}$$
$$(1, -s^{(m)}, 0) w^{(m)} = g^{(m)}\,. \tag{6.77}$$

In terms of the characteristic variables in the directions $t = (n+m)/\sqrt{2}$, at the corner we have the following two conditions

$$(1, -s^{(n)}, 0) R(n,t) w^{(t)} = g^{(n)}\,, \tag{6.78}$$
$$(1, -s^{(m)}, 0) R(m,t) w^{(t)} = g^{(m)}\,. \tag{6.79}$$

Using the fact that $t = (n+m)/\sqrt{2}$ and $n \cdot m = n_i m_j \delta^{ij} = 0$, the matrix $R(t,n)$ becomes

$$R(n,t) = \begin{pmatrix} \frac{1}{2}(1+\frac{1}{\sqrt{2}}) & \frac{1}{2}(1-\frac{1}{\sqrt{2}}) & -\frac{1}{2} m \cdot n^{\perp} \\ \frac{1}{2}(1-\frac{1}{\sqrt{2}}) & \frac{1}{2}(1+\frac{1}{\sqrt{2}}) & \frac{1}{2} m \cdot n^{\perp} \\ \frac{1}{2} m \cdot n^{\perp} & -\frac{1}{2} m \cdot n^{\perp} & \frac{1}{\sqrt{2}} \end{pmatrix}. \tag{6.80}$$

Similarly, the matrix $R(m,t)$ can be obtained from the one above by exchanging n with m. The two boundary conditions become

$$\left(\frac{1 - s^{(n)}}{2} + \frac{1 + s^{(n)}}{2\sqrt{2}} \right) w^{(+1;t)} + \left(\frac{1 - s^{(n)}}{2} - \frac{1 + s^{(n)}}{2\sqrt{2}} \right) w^{(-1;t)}$$
$$-\delta \frac{1 + s^{(n)}}{2} w^{(0;t)} = g^{(n)}\,,$$
$$\left(\frac{1 - s^{(m)}}{2} + \frac{1 + s^{(m)}}{2\sqrt{2}} \right) w^{(+1;t)} + \left(\frac{1 - s^{(m)}}{2} - \frac{1 + s^{(m)}}{2\sqrt{2}} \right) w^{(-1;t)}$$
$$+\delta \frac{1 + s^{(m)}}{2} w^{(0;t)} = g^{(m)}\,,$$

where $\delta = m \cdot n^{\perp}$. If $s^{(n)} \neq -1$ and $s^{(m)} \neq -1$, then one can solve for the ingoing and the zero speed modes. By multiplying the first equation by $(1+s^{(m)})$ and the second equation by $(1+s^{(n)})$ and taking the sum, we get

$$\begin{aligned}
&\left(1 - s^{(n)}s^{(m)} + \frac{(1+s^{(n)})(1+s^{(m)})}{\sqrt{2}}\right) w^{(+1;t)} + \\
&\left(1 - s^{(n)}s^{(m)} - \frac{(1+s^{(n)})(1+s^{(m)})}{\sqrt{2}}\right) w^{(-1;t)} = \\
&= (1+s^{(n)})g^{(m)} + (1+s^{(m)})g^{(n)}\,. \qquad (6.81)
\end{aligned}$$

A different linear combination gives

$$\begin{aligned}
&\delta\left(1 - s^{(n)}s^{(m)} + \frac{(1+s^{(n)})(1+s^{(m)})}{\sqrt{2}}\right) w^{(0;t)} + \sqrt{2}(s^{(n)} - s^{(m)})w^{(-1;t)} = \\
&\left(1 - s^{(n)} + \frac{1+s^{(n)}}{\sqrt{2}}\right) g^{(m)} - \left(1 - s^{(m)} + \frac{1+s^{(m)}}{\sqrt{2}}\right) g^{(n)}\,. \qquad (6.82)
\end{aligned}$$

The first equation can be solved for the ingoing mode $w^{(+1;t)}$ and does not contain the zero speed mode. The coupling between the ingoing mode, $w^{(+1;t)}$, and the outgoing mode, $w^{(-1;t)}$, is never greater than 1 in magnitude. The second equation can be solved for $w^{(0;t)}$. In this case, however, the coupling to the outgoing mode is not necessarily bounded by 1. Notice that for $s^{(n)} = s^{(m)} \neq -1$ the outgoing mode disappears from the second equation.

We now list some particular cases of (6.81) and (6.82), which might be useful for the linearized GEC system.

For $s^{(n)} = s^{(m)} = 0$ we get

$$\begin{aligned}
w^{(+1;t)} &= (2\sqrt{2}-3)w^{(-1;t)} + (2-\sqrt{2})(g^{(n)} + g^{(m)})\,, \qquad (6.83)\\
w^{(0;t)} &= \delta(g^{(m)} - g^{(n)})\,. \qquad (6.84)
\end{aligned}$$

For $s^{(n)} = s^{(m)} = 1$ we get

$$\begin{aligned}
w^{(+1;t)} &= w^{(-1;t)} + (g^{(n)} + g^{(m)})/\sqrt{2}\,, \qquad (6.85)\\
w^{(0;t)} &= \delta(g^{(m)} - g^{(n)})/2\,. \qquad (6.86)
\end{aligned}$$

For $s^{(n)} = 1$ and $s^{(m)} = -1$ we get

$$\begin{aligned}
w^{(+1;t)} &= -w^{(-1;t)} + g^{(m)}\,, \qquad (6.87)\\
w^{(0;t)} &= -\sqrt{2}\delta w^{(-1;t)} + \delta(g^{(m)}/\sqrt{2} - g^{(n)})\,. \qquad (6.88)
\end{aligned}$$

For $s^{(n)} = -1$ and $s^{(m)} = 1$ we get

$$w^{(+1;t)} = -w^{(-1;t)} + g^{(n)}\,, \tag{6.89}$$
$$w^{(0;t)} = \sqrt{2}\delta w^{(-1;t)} - \delta(g^{(n)}/\sqrt{2} - g^{(m)})\,. \tag{6.90}$$

For $s^{(n)} = 1$ and $s^{(m)} = 0$ we get

$$w^{(+1;t)} = (3 - 2\sqrt{2})w^{(-1;t)} + (\sqrt{2} - 1)(g^{(n)} + 2g^{(m)})\,, \tag{6.91}$$
$$w^{(0;t)} = (\sqrt{2} - 2)\delta w^{(-1;t)} - \delta g^{(n)}/\sqrt{2} + (2 - \sqrt{2})\delta g^{(m)}\,. \tag{6.92}$$

For $s^{(n)} = -1$ and $s^{(m)} = 0$ we get

$$w^{(+1;t)} = -w^{(-1;t)} + g^{(n)}\,, \tag{6.93}$$
$$w^{(0;t)} = \sqrt{2}\delta w^{(-1;t)} - \left(1 + \frac{1}{\sqrt{2}}\right)\delta g^{(n)} + 2\delta g^{(m)}\,. \tag{6.94}$$

Finally, for $s^{(n)} = s^{(m)} = -1$ we get

$$w^{(+1;t)} = -w^{(-1;t)} + g^{(n)}\,. \tag{6.95}$$

When dealing with a system such as the wave equation, setting to zero the incoming modes at the boundary is a reasonable approximation to a radiative boundary condition. In addition to some initial data with compact support, it may be tempting to specify, at the numerical level, boundary conditions that correspond to setting the incoming modes everywhere to zero, including the ones at the corners. According to (6.83), setting the incoming mode in the direction t at the corner to zero will lead, in general, to an inconsistency. The numerical experiments of the next section will clarify this point.

6.4 Experiments with the Wave Equation

In this section we perform numerical experiments aimed at determining (i) what type of boundary data should be specified at the corner and (ii) which compatibility conditions should be enforced to avoid losing the desired order of accuracy. To tackle the first point we need to isolate it from the second.

To ensure that the compatibility conditions at the corners are automatically satisfied we give vanishing boundary data in a neighborhood of the corners. Numerical stability can be obtained by giving data to the incoming mode at 45 degrees. However, since data is provided at the two intersecting faces, it is important that what is done

at the corner is consistent. We claim that, for the case of the wave equation, data should be given to both the incoming mode (appropriately coupled to the outgoing one) and the zero speed mode as illustrated in the previous section.

As usual, we reduce the wave equation to a two dimensional problem by assuming no dependence on the independent variable z. We use the domain $\Omega = [0,1] \times [0,1]$ and give zero initial data and zero boundary data to the incoming fields everywhere except at the face $x = 0$, where we set

$$w^{(+1;n)} = \sin^4(2\pi t) \sin^4(2\pi(y - 1/4)) \tag{6.96}$$

for $1/4 < y < 3/4$ and $0 \leq t$. We are essentially injecting a periodic pulse through the boundary.

The convergence rate of the constraint at the boundary when the 45 degree modes at the boundary are set to zero is shown in Fig. 6.1. The loss of convergence is a symptom of lack of consistency. This is supported by the fact that the maximum of the discretized constraint is not converging to zero, see Fig. 6.2.

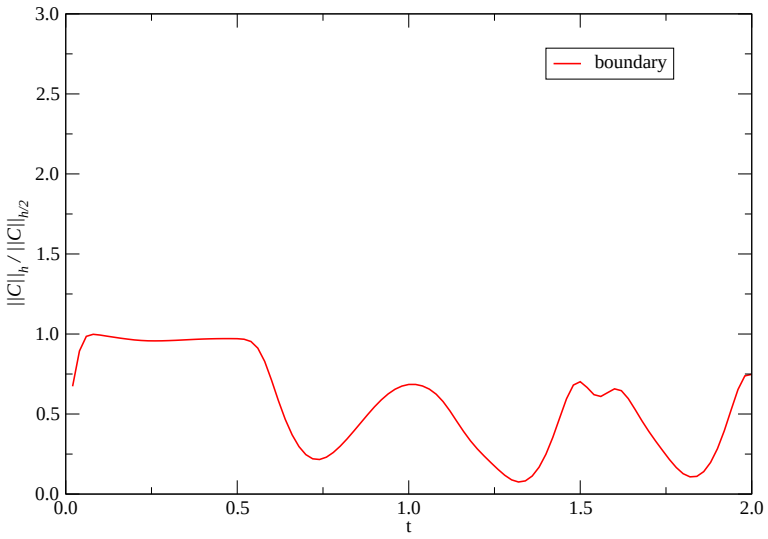

Figure 6.1: The convergence rate of the discrete constraint $C_{ij} \equiv D^{(y)}X_{ij} - D^{(x)}Y_{ij}$ at the boundary. The lack of convergence is a strong indication that setting to zero the incoming modes at 45 degrees at the corners is inconsistent.

If, however, the coupling (6.83) is used, there is a noticeable improvement. See Fig. 6.3 and 6.4.

Although at the interior of a face, giving data to a zero speed modes means that one is overdetermining the system, numerical experiments seem to suggest that at

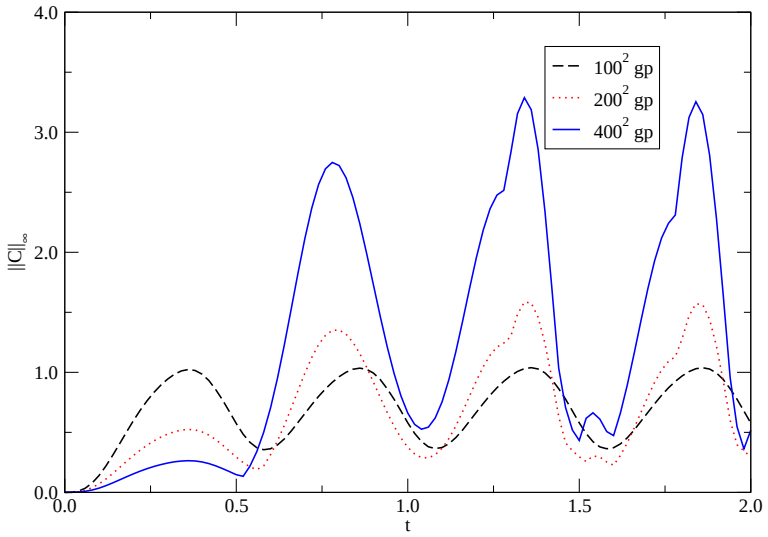

Figure 6.2: The L_∞ norm of the discrete constraint reveals that there are gridpoints at which the constraint is not converging to zero.

the corner of a computational domain this can and should be done. From Fig. 6.5 and 6.6 we see that if the zero speed mode is also overwritten, then the constraint is of order $\mathcal{O}(h)$ at the corner.

We now look at the compatibility issue. If we use the following boundary data ($s^{(n)} = s^{(m)} = 0$)

$$g^{(n)}(t,y) = (1+\cos(4\pi y))^2 \sin^4(2\pi t)\,, \qquad y \leq 1/4\,, \tag{6.97}$$

$$g^{(m)}(t,x) = 0\,, \tag{6.98}$$

the compatibility condition (6.8) is violated. Fig. 6.7 illustrates what happens to the constraints at the corner when incompatible data is used.

6.5 Experiments with the Neumann and Dirichlet Cases

In this section we review and analyze the proposal of [8] for the handling of corners. The domain is $\Omega = [0,1] \times [0,1]$.

- **Neumann**

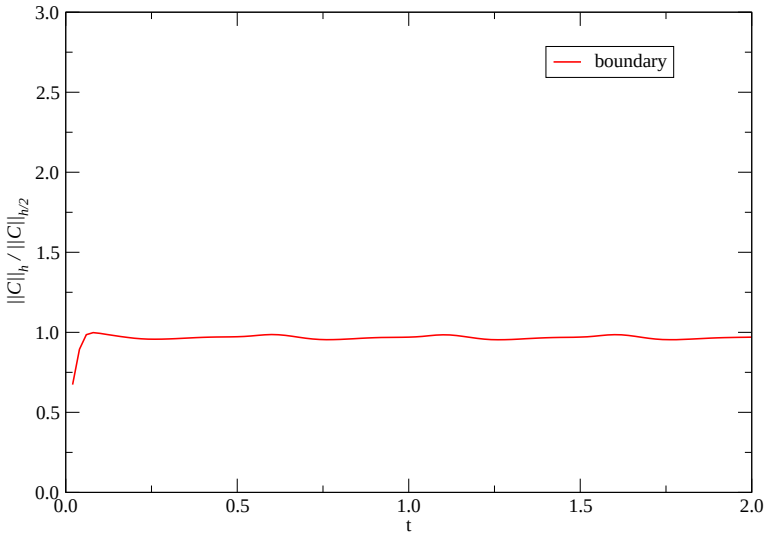

Figure 6.3: The convergence rate of the discrete constraint $C_{ij} \equiv D^{(y)}X_{ij} - D^{(x)}Y_{ij}$ at the boundary for $h = 1/100$. The coupling (6.83) between in and out-going modes was used.

In [8] it was suggested that, for the Neumann case, at an edge of the computational domain, in addition to specifying the source terms, one should give data to K_{nm}, where n and m are the normals of the two intersecting faces. This was obtained by analyzing the closed systems at two adjacent faces and by observing that the characteristic variables of the boundary system in the direction m (m is orthogonal to n, $\delta^{ij}m_i n_j = 0$, and therefore tangential to the boundary face) are given by

$$\begin{aligned} w^{(\pm\sqrt{3/2};m)} &= \pm K_{nm} - \sqrt{\frac{2}{3}}\left[(1+\kappa)f_{mmn} + \kappa f_{ppn} - \left(\kappa - \frac{1}{2}\right)(f_{nmm} + f_{npp})\right], \\ w^{(\pm 1;m)} &= \pm K_{np} - f_{mpn}\,, \end{aligned}$$

where p is orthogonal to n and m, $\delta^{ij}p_i n_j = \delta^{ij}p_i m_j = 0$.

Giving data to K_{nm} at the edge automatically ensures that the zeroth order and the first two compatibility conditions (6.23) and (6.24) are satisfied.

We also notice that conditions (6.25)–(6.28) are part of the closed system and therefore will be satisfied. On the other hand, the last condition (6.29) is not part of the closed system and is not automatically satisfied. In fact, it is easy

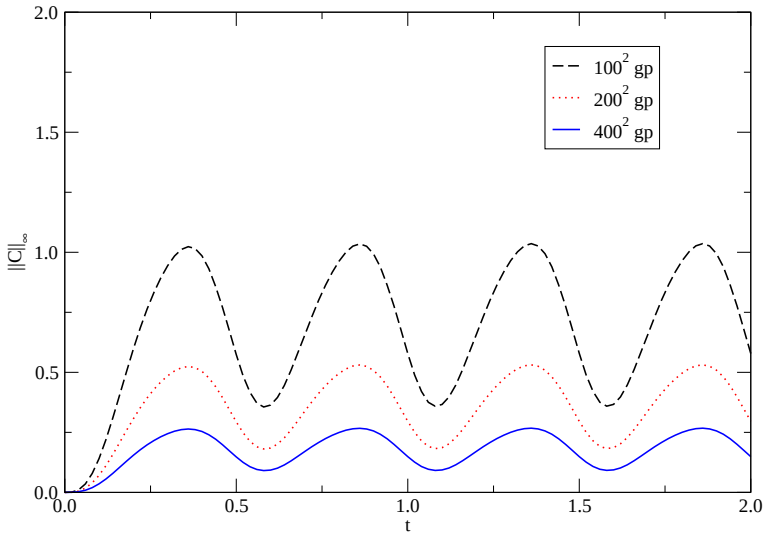

Figure 6.4: The L_∞ norm of the discrete constraint.

to give data to the source terms so that this condition is violated. For example, if we give vanishing initial data and set all source terms to zero, apart from

$$g^{(n)}_{nn}(t,y) = \sin^4(2\pi t)\sin(2\pi y)\,, \qquad 0 \le t \le 1\,, \tag{6.99}$$

at $x = 0$, we obtain Figs. 6.8 and 6.9, confirming that the first order compatibility condition (6.29) is violated.

Neglecting the problem of the incompatible source terms, the discretization appears to be stable. Fig. 6.10 shows a convergence test for the Hamiltonian constraint with $\eta = 1$.

- **Dirichlet**

  In the Dirichlet case the characteristic variables of the boundary system in the direction m, orthogonal to n, are

$$w^{(\pm\sqrt{3/2};m)} = \pm K_{BB} - \sqrt{\frac{2}{3}}\left((1+\kappa)f_{nnm} + h_m\right). \tag{6.100}$$

  The source terms on both faces provide the necessary data at the edge.

  As in the Neumann case, it is possible to give data to the source terms so that one of the first order compatibility conditions is violated. For example, if we

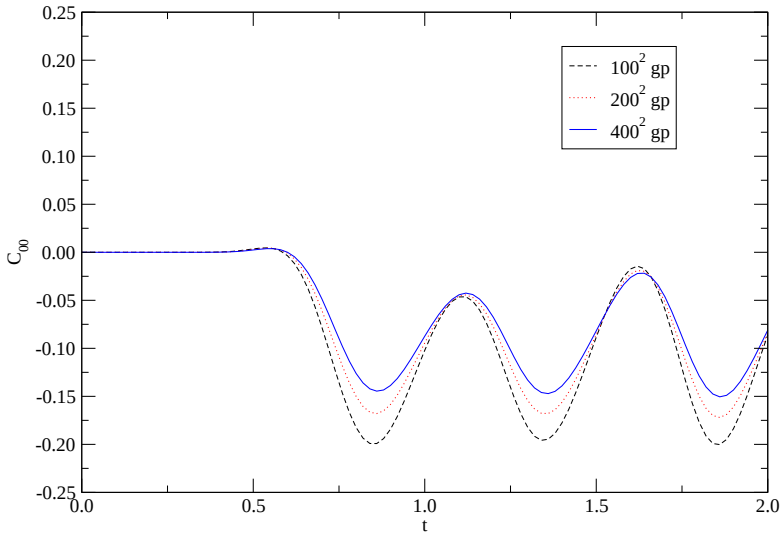

Figure 6.5: The value of the discrete constraint at the corner, $C_{00} = D_+^{(y)} X_{00} - D_+^{(x)} Y_{00}$, if the zero speed mode is not overwritten.

give vanishing initial data and set all the source terms to zero apart from

$$g_{mp}^{(n)}(t, y) = \sin^4(2\pi t) \sin(2\pi y)\,, \qquad 0 \le t \le 1\,, \tag{6.101}$$

at $x = 0$, we obtain the plot of Fig. 6.11.

Notice that in neither the Neumann nor the Dirichlet case is data given in the 45 degree direction.

6.6 Experiments with the Sommerfeld Case

There does not seem to be a preferred way of treating the corners in the Sommerfeld case. Whereas in the Neumann and Dirichlet cases the existence of a closed system at the boundary has proved helpful for the handling of the corners, in the Sommerfeld case such a closed system cannot be constructed. Again, we resort to numerical experimentation to establish which boundary conditions lead to a stable or unstable scheme.

Let us assume that n and m are the normals of the two (orthogonal) faces that meet at an edge. We denote by $t = (n + m)/\sqrt{2}$ the normal at 45° and $b = \delta(m - n)/\sqrt{2}$, where $\delta = n^\perp \cdot m$, a unit vector orthogonal to t. At the edge we use equations (5.5)–(5.6) with n replaced by t. We define the tangential directions to be the directions

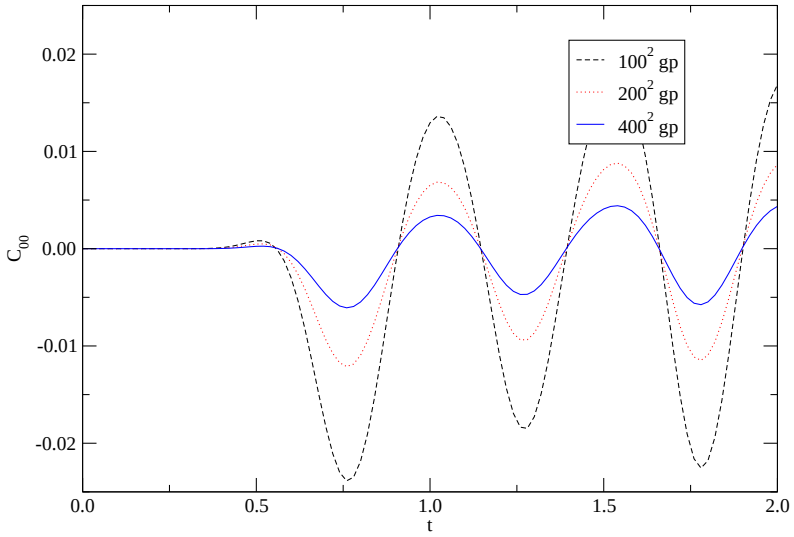

Figure 6.6: The value of the discrete constraint at the corner, $C_{00} = D_+^{(y)} X_{00} - D_+^{(x)} Y_{00}$, if the zero speed mode is overwritten. In this case it is of order $\mathcal{O}(h)$.

orthogonal to t. Unfortunately, Fig. 6.12 shows that the resulting scheme is unstable and suffers from exponential growth of the error.

6.6.1 An Alternative Implementation

The lack of success in the Sommerfeld case and the compatibility issues encountered in the Neumann and Dirichlet cases clearly illustrate the difficulty associated with non-smooth boundaries and make the idea of using smooth boundaries more attractive.

Assume that $\partial\Omega$ is the smooth boundary of the bounded set Ω. Locally, one can choose a coordinate system adapted to this boundary, i.e., $\partial\Omega$ is given by the set of points in which one of the coordinates is constant. An alternative implementation of the Sommerfeld case consists in setting the incoming constraint variable to zero for $\eta \in (0, 8/3)$. The system will have lower order terms and non-constant coefficients. The experience gained in this work makes it conceivable that the resulting problem can be discretized in a stable manner using, for example, overlapping grids to cover the entire domain.

Moreover, one could also try to modify the evolution equations by appropriately adding constraints to the right hand side, such that the constraints propagate tangentially to the boundary. This technique was used in [10] and heavily relies on the fact that the boundary is smooth. For metric formulations one might expect to lose

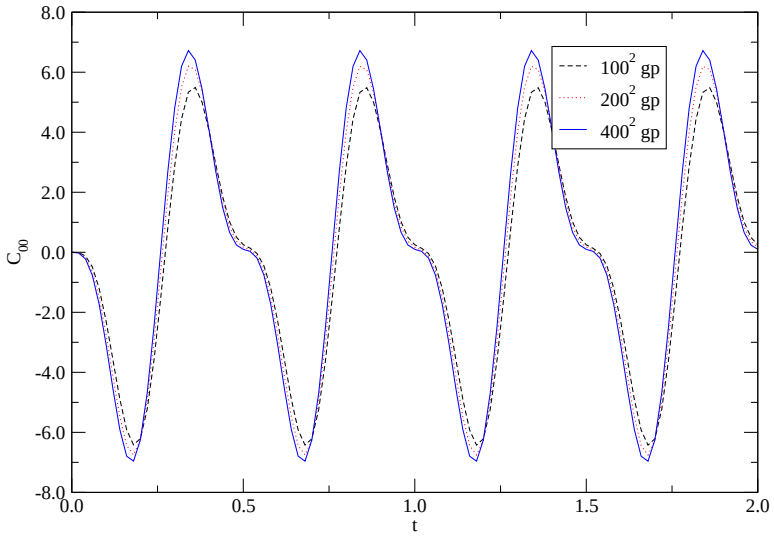

Figure 6.7: The value of the discrete constraint at the corner, $C_{00} = D_+^{(y)} X_{00} - D_+^{(x)} Y_{00}$, when incompatible boundary data is used. The error is clearly of order $\mathcal{O}(1)$.

symmetric hyperbolicity. This will be analyzed further in a future work.

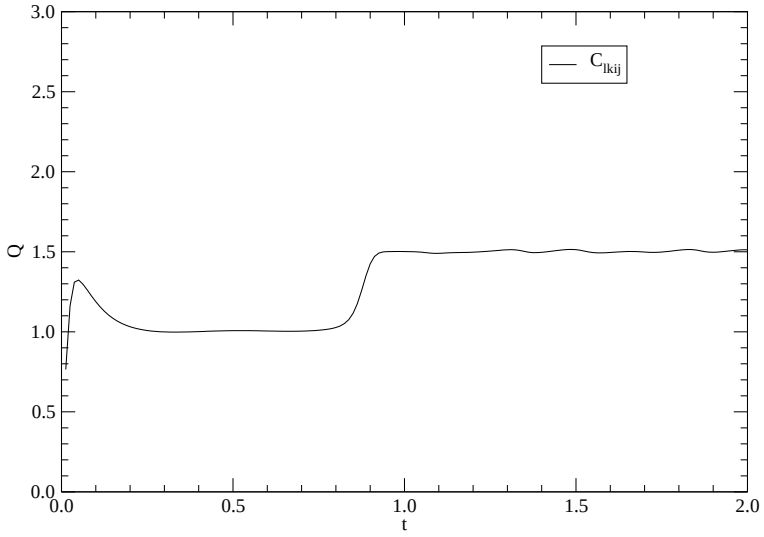

Figure 6.8: The reduced order of convergence for the Euclidean L_2 norm of the four index constraints confirms that with the boundary data (6.99) one of the first order compatibility conditions, Eq. (6.29), is not satisfied in the Neumann case.

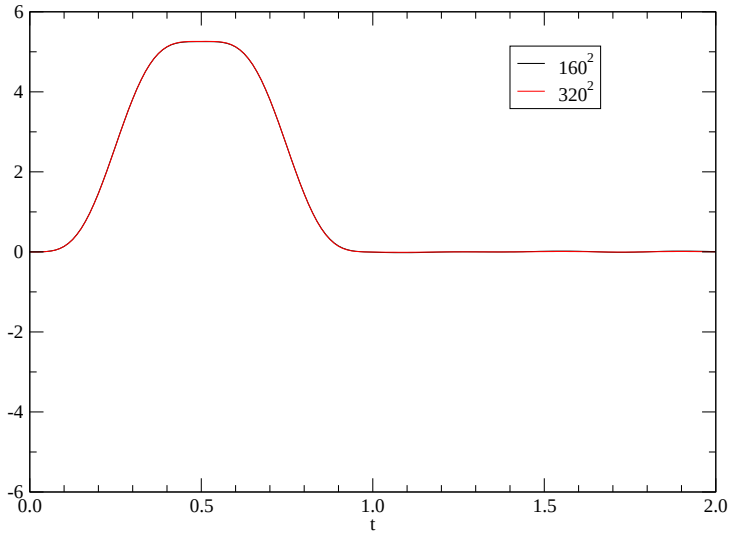

Figure 6.9: This figure show that with the boundary data (6.99) the $\tilde{C}_{nm}$ defined in (6.13) at the corner $(x, y) = (0, 0)$ is of order $\mathcal{O}(1)$. The two curves overlap.

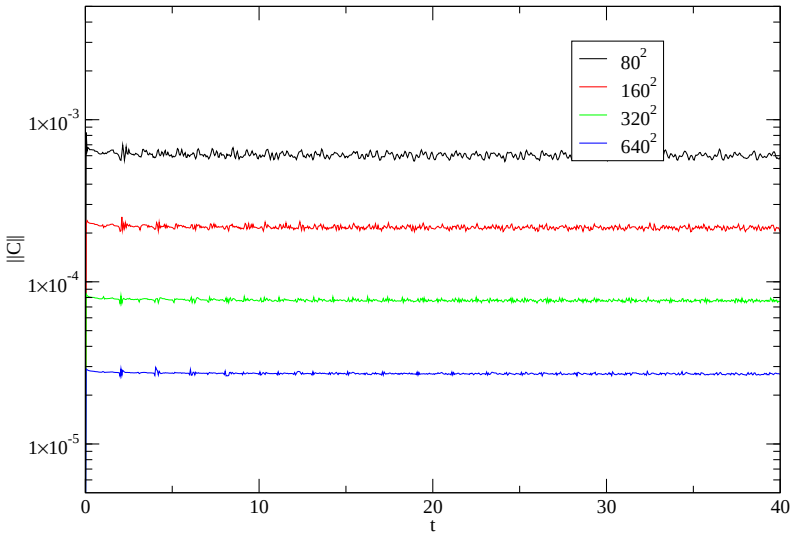

Figure 6.10: The Hamiltonian constraint is convergent for Neumann boundary conditions in the presence of corners. The initial data and the source terms are given to reproduce a gauge wave traveling in the direction $d = (+1, +1, 0)/\sqrt{2}$.

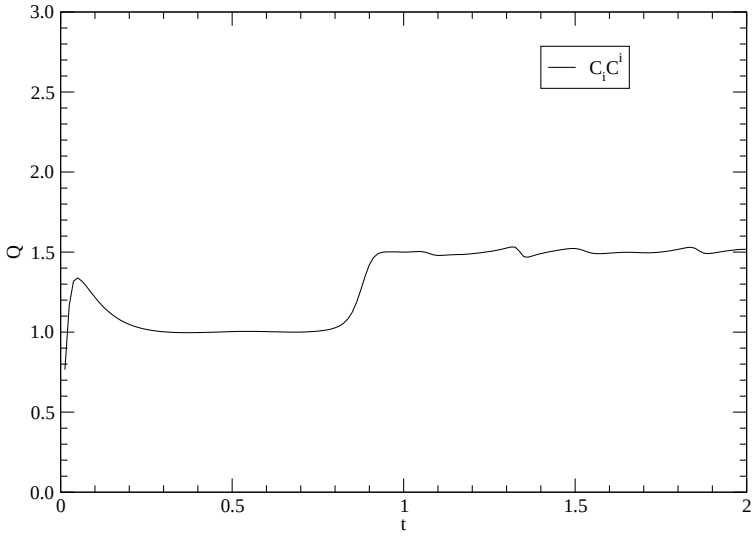

Figure 6.11: The reduced order of convergence for the momentum constraints confirms that with the boundary data (6.101) one of the first order compatibility conditions, Eq. (6.51), for the Dirichlet case is not satisfied.

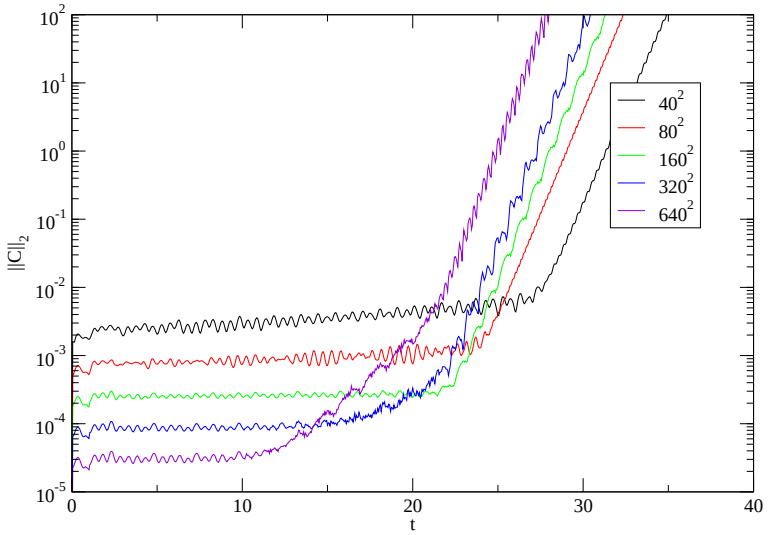

Figure 6.12: Setting the ingoing constraints in the $t = (n + m)/\sqrt{2}$ direction to zero leads to an unstable scheme. This figure shows the L_2 norm of the Hamiltonian constraint at different resolutions for a gauge wave traveling in the direction $d = (+1, +1, 0)/\sqrt{2}$ with $\eta = 1$. Although the exponential rate of growth appears to be the same, the growth begins sooner as the resolution is increased.

Chapter 7

Summary and Results

Einstein's field equations can be split into evolution equations and constraint equations. When solving the evolution equations in a portion of space-time with time-like boundaries, one is essentially dealing with an initial-boundary value problem. In this work we confined ourselves to strongly hyperbolic formulations, first order in time and space. In particular, we chose the generalized Einstein-Christoffel system linearized about Minkowski in Cartesian coordinates, precisely the same system used in [8] and [9]. Within this formulation, the constraints represent equations involving spatial derivatives of the main variables. An issue that has not been adequately addressed in the past, but which is gradually receiving more attention, is that the constraints, in addition to reducing the freedom that one has in the specification of the initial data, restrict the choice of boundary data that one can prescribe to the incoming variables. To determine the nature of this restriction we followed the method used in [8] and [9], based on the characteristic analysis of the evolution of the constraint variables. This leads to constraint-preserving boundary conditions.

In addition to the Neumann and Dirichlet cases that were presented in [8], we looked at the Sommerfeld case. What makes the Sommerfeld case more attractive than the first two, is the fact that, if it can be implemented in a stable way, it would provide a good approximation to radiative, constraint-preserving boundary conditions. Consequently, it would be an excellent candidate for the simulation of isolated sources. The only result available for this case was the one presented in [9], where it was proved that, if the free parameter associated with the family of formulations lies outside a certain range, then the problem is ill-posed. Unfortunately, it does not shed any light on cases in which the parameter lies inside this range.

By making certain symmetry assumptions we eliminated one of the spatial dimensions from the problem. This proved to be an invaluable method for the investigation of the stability properties of the discretizations of various boundary conditions. The

major result of this work was the numerical implementation of the linearized Einstein's equations with constraint-preserving boundary conditions. A great number of numerical experiments were conducted and several results of [8] and [9] were confirmed, such as the well-posedness of the Neumann and Dirichlet cases with a smooth boundary. Furthermore, the results clearly suggested that there exists a range of values in the parameter space in which the Sommerfeld case can be discretized in a stable way. Unfortunately the last result seems to hold only in the case of a smooth boundary, i.e., we were not able to find a stable discretization in the presence of corners. The analysis also revealed that, in the Neumann and Dirichlet cases with corners, although stability can be obtained, data to the source has to be given with great care in order to avoid violating compatibility conditions of higher order, which were not taken into account in [8].

Modulo corners, the result obtained with the Sommerfeld case opens a new window of possibilities. Provided that one can avoid non-smooth domains, it may very well be that Sommerfeld constraint-preserving boundary conditions would work in the fully non-linear case. This is an issue that certainly merits further investigation.

This work forced us to look deeply into the problems that arise when discretizing a system in the presence of corners. It revealed that, although stability results exists for maximally dissipative boundary conditions, more needs to be done in order to achieve consistency. For example, even for the simple case of the wave equation on a flat background, setting the incoming modes to zero, including the one at the corner, is inconsistent. In this work we showed that, to avoid such inconsistency, a certain combination of in- and outgoing variables should be specified at the corner. An aspect of the problem which was not studied was the presence of vertices, as the symmetry assumption in the numerical implementation only allowed for edges. More work needs to be done to investigate this issue.

It is important to realize that no finite number of numerical experiments can replace an analytical proof of stability. However, in most situations a proof of stability for the system of interest would be a formidable challenge. It is in these situations that careful experimentation, especially on simple toy models, could be used, particularly to rule out unstable schemes.

Chapter 8

Conclusion

Despite the success in the stable discretization of the Neumann and Dirichlet cases we feel that such systems are inadequate in terms of their ability to simulate isolated sources. The coupling between in- and outgoing modes required by these boundary conditions is such that reflections are essentially guaranteed. The Sommerfeld case, on the other hand, has proven to be applicable to the smooth boundary case, but not when corners are present. Although it might be possible to improve on this by further investigating the problem, we believe that smooth boundaries are preferable anyway. Implementing a smooth boundary in three dimensions is not trivial. A technique that is increasingly receiving more and more attention is based on overlapping grids, which would not only allow for smooth boundaries, but also for moving boundaries, see [17, 33]. The advantages that a smooth boundary provides outweigh the technical difficulties involved in the implementation of overlapping grids.

The construction of well-posed constraint-preserving boundary conditions for metric formulations of Einstein's equations still needs to be improved. So far well-posedness proofs are only available for a few particular cases, such as those proposed in [8] and [14]. It is conceivable that using the theory of pseudodifferential operators might lead to well-posedness proofs for the linear variable coefficient case. However, preliminary work [34] seems to suggest that this would be prohibitively difficult.

As this dissertation is being completed, Nagy and Sarbach [35] are investigating modifications of the Friedrich and Nagy work [10], the best result obtained so far concerning the well-posedness of the initial-boundary value problem for the full Einstein vacuum equations. The main difference lies in the gauge condition for the tetrad. Whereas in [10] the tetrad is such that one of the vectors is tangential to the time-like boundary surface and another one is adapted to the the outward unit normal, in the recent work of Nagy and Sarbach the last condition is relaxed. As a consequence, their equations are somewhat simpler. To prevent constraint-violating

modes from entering the domain, they follow the idea of [10], where constraints are added to the right hand side so that, at the boundary, the constraints propagate along the boundary. Both the main evolution system and the evolution of the constraints system are symmetric hyperbolic.

As progress is made in the research of boundary conditions for numerical relativity, we will be better able to judge whether constraint-preserving boundary conditions for metric or tetrad formulations of Einstein's equations will improve the life-time of numerical simulations.

Bibliography

[1] R.A. Hulse and J.H. Taylor, Ap. J. Lett. **195**, L51 (1975); J.H. Taylor and J.M. Weisberg, Ap. J. **253**, 908 (1982); J.M. Weisberg and J.H. Taylor, Phys. Rev. Lett. **52**, 1348 (1984).

[2] L. Lehner, Class. Quantum Grav. **18**, R25 (2001).

[3] O. Reula, Hyperbolic Methods for Einstein's Equations, Living Rev. Relativity 1, 3 (1998): `http://www.livingreviews.org/lrr-1998-3`.

[4] L.E. Kidder, M.A. Scheel, and S.A. Teukolsky, Phys. Rev. D **64**, 064017 (2001).

[5] Y. Choquet-Bruhat and J.W. York, Lect. Notes Phys. **592**, 29–58 (2002).

[6] O. Brodbeck, S. Frittelli, P. Hübner, and O.A. Reula, J. Math. Phys. **40**, 909 (1999).

[7] P. Olsson, Math. Comp. **64**, 1035 (1995); **64**, S23 (1995); **64**, 1473 (1995).

[8] G. Calabrese, J. Pullin, O. Reula, O. Sarbach, and M. Tiglio, Commun. Math. Phys. **240**, 377–395 (2003).

[9] G. Calabrese and O. Sarbach, J. Math. Phys. **44**, 3888–3899 (2003).

[10] H. Friedrich and G. Nagy, Comm. Math. Phys. **201**, 619 (1999).

[11] J.M. Stewart, Class. Quantum Grav. **15**, 2865 (1998).

[12] S. Frittelli and O.A. Reula, Phys. Rev. Lett. **76**, 4667 (1996).

[13] G. Calabrese, L. Lehner, and M. Tiglio, Phys. Rev. D **65**, 104031 (2002).

[14] B. Szilágyi and J. Winicour, Phys. Rev. D **68**, 041501 (2003).

[15] S. Frittelli and R. Gómez, Class. Quant. Grav. **20**, 2379–2392 (2003).

[16] S. Frittelli and R. Gómez, Phys. Rev. D **68**, 044014 (2003).

[17] G. Calabrese and D. Neilsen, *Spherical excision for moving black holes and summation by parts for axisymmetric systems*, arXiv:gr-qc/0308008

[18] B. Strand, J. Comp. Phys. **110**, 47 (1994).

[19] J. Hadamard, *Sur les problèmes aux derivées partielles et leur signification physique*, Bull. Univ. Princeton **13**, 49–52 (1902).

[20] A.N. Tikhonov and A.V. Goncharsky, *Ill-posed problems in the natural sciences* (MIR, Moscow, 1987).

[21] H.O. Kreiss, J. Lorenz, *Initial-Boundary Value Problems and the Navier-Stokes Equations*, (Academic, New York, 1989).

[22] B. Gustafsson, H. Kreiss, and J. Oliger, *Time dependent problems and difference methods*, (Wiley, New York, 1995).

[23] D. Givoli, J. Comput. Phys. **94**, 1–29 (1991).

[24] A. Sommerfeld, *Lectures on Theoretical Physics*, (Academic, New York, 1964).

[25] P.D. Lax, and R.S. Phillips, Commun. Pure Appl. Math. **13**, 427 (1960).

[26] R. Wald, *General Relativity* (University of Chicago Press, Chicago, 1984).

[27] R. Arnowitt, S. Deser, and C. Misner, in *Gravitation: An Introduction to Current Research*, edited by L. Witten (Wiley, New York, 1962).

[28] J.W. York, in *Sources of Gravitational Radiation*, edited by L. Smarr (Cambridge University Press, Cambridge, 1979).

[29] O. Sarbach and M. Tiglio, Phys. Rev. D **66**, 064023 (2002).

[30] A. Anderson and J.W. York, Jr., Phys. Rev. Lett. **82**, 4384 (1999).

[31] G. Calabrese, L. Lehner, O. Reula, O. Sarbach, and M. Tiglio, *Summation by parts and dissipation for domains with excised regions*, arXiv:gr-qc/0308007 (2003).

[32] M.W. Choptuik, Phys. Rev. D **44**, 3124 (1991).

[33] J. Thornburg, Class. Quantum Grav. **4**, 1119 (1987).

[34] G. Nagy and O. Sarbach, private communication.

[35] G. Nagy and O. Sarbach, in preparation.

Appendix A

Basic Properties of Finite Difference Operators

In this appendix the definition and some important properties of the finite difference operators D_+, D_- and D_0 are given. For a proof see [22].

For simplicity assume that the domain is the compact set $\Omega = [0, 1]$. Introduce gridpoints $x_j = jh$, $j = 0, 1, \ldots, N$ with $h = 1/N$ and a grid function $u_j = u(x_j)$. By definition,

$$\begin{aligned} D_+u_j &= (u_{j+1} - u_j)/h\,, \qquad \text{for } j = 0, 1, \ldots, N-1\,, \\ D_-u_j &= (u_j - u_{j-1})/h\,, \qquad \text{for } j = 1, 2, \ldots, N\,, \\ D_0u_j &= (u_{j+1} - u_{j-1})/(2h)\,, \qquad \text{for } j = 1, 2, \ldots, N-1\,. \end{aligned}$$

Immediate consequences are

$$\begin{aligned} u_j &= \mp hD_\pm u_j + u_{j\pm1}\,, \\ D_0 &= (D_+ + D_-)/2\,, \\ D_\pm u_j &= D_\mp u_{j\pm1}\,, \\ D_+D_-u_j &= D_-D_+u_j = (u_{j+1} - 2u_j + u_{j-1})/h^2\,, \\ (D_+D_-)^2u_j &= (u_{j+2} - 4u_{j+1} + 6u_j - 4u_{j-1} + u_{j-2})/h^4\,. \end{aligned}$$

Furthermore, if $v_j = v(x_j)$, where v is a smooth function, then

$$\begin{aligned} D_\pm v_j &= v'(x_j) \pm \frac{1}{2}v''(x_j)h + \mathcal{O}(h^2)\,, \\ D_0v_j &= v'(x_j) + \frac{1}{6}v'''(x_j)h^2 + \mathcal{O}(h^4)\,, \end{aligned}$$

$$
\begin{aligned}
D_+D_-v_j &= v''(x_j) + \frac{1}{12}v^{(4)}(x_j)h^2 + \mathcal{O}(h^4)\,, \\
(D_+D_-)^2v_j &= v^{(4)}(x_j) + \frac{1}{6}v^{(6)}(x_j)h^2 + \mathcal{O}(h^4)\,.
\end{aligned}
$$

With respect to the scalar product and norm

$$
(u,v)_{r,s} = \sum_{j=r}^{s} u_j v_j h, \qquad \|u\|_{r,s}^2 = (u,u)_{r,s}
$$

the difference operators satisfy the following properties:

$$
\begin{aligned}
(u, D_+v)_{r,s} &= -(D_-u, v)_{r+1,s+1} + u_j v_j|_r^{s+1} \\
&= -(D_+u, v)_{r,s} - h(D_+u, D_+v)_{r,s} + u_j v_j|_r^{s+1}\,, \\
(u, D_-v)_{r,s} &= -(D_+u, v)_{r-1,s-1} + u_j v_j|_{r-1}^{s} \\
&= -(D_-u, v)_{r,s} + h(D_-u, D_-v)_{r,s} + u_j v_j|_{r-1}^{s}\,, \\
(u, D_0v)_{r,s} &= -(D_0u, v)_{r,s} + \frac{1}{2}(u_j v_{j+1} + \bar{u}_{j+1} v_j)|_{r-1}^{s}\,.
\end{aligned}
$$

Appendix B

A Differential Inequality

Let y be a differentiable function of t. If

$$\frac{dy}{dt} \leq ay(t) + f(t) \tag{B.1}$$

then

$$y(t) \leq y(0) + \int_0^t e^{a(t-\tau)} f(\tau) d\tau \,. \tag{B.2}$$

To prove this (see [21]) we introduce $z(t) = e^{-at} y(t)$ and observe that

$$\frac{dz}{dt} = -az + e^{-at} \frac{dy}{dt} \leq e^{-at} f(t) \,.$$

Integrating, we get

$$z(t) - z(0) \leq \int_0^t e^{-a\tau} f(\tau) d\tau \,.$$

Using the definition of $z(t)$ we get (B.2).

Appendix C

Inhomogeneous Boundary Conditions

We analyze inhomogeneous boundary conditions in a simple problem using Olsson's method and compute the discrete energy estimate.

Consider the scalar model problem

$$\frac{\partial u}{\partial t} = \frac{\partial u}{\partial x}\,, \qquad 0 \le x \le 1\,, \quad t \ge 0\,, \tag{C.1}$$

$$u(0,x) = f(x)\,, \tag{C.2}$$

$$u(t,1) = g(t)\,, \tag{C.3}$$

with real solution u. The initial and boundary data are smooth and satisfy the compatibility conditions $d^n g/dt^n(0) = d^n f/dx^n(1)$ for $n = 0, 1, 2, \ldots$.

The time derivative of the energy

$$E(t) = \int_0^1 u^2(t,x)dx$$

gives

$$\frac{d}{dt}E = g(t)^2 - u(t,0)^2\,. \tag{C.4}$$

Consider now the semi-discrete approximation

$$\frac{dv_0}{dt} = D_+ v_0\,, \tag{C.5}$$

$$\frac{dv_j}{dt} = D_0 v_j\,, \qquad j = 1, \ldots, N-1\,, \tag{C.6}$$

$$\frac{dv_N}{dt} = \frac{dg}{dt}\,, \tag{C.7}$$

$$v_j(0) = f(x_j)\,, \tag{C.8}$$

where $x_j = hj$ with $h = 1/N$. Notice that, as a consequence of the compatibility condition, $g(0) = f(1)$, we have that $v_N(t) = g(t)$ for all $t \geq 0$. We define the discrete energy to be

$$E = (v, v)_h = \frac{h}{2} v_0^2 + h \sum_{j=1}^{N-1} v_j^2 + \frac{h}{2} v_N^2 \,. \tag{C.9}$$

Its time derivative gives

$$\frac{d}{dt} E = -v_0^2 + v_{N-1} g + hg \frac{dg}{dt} = -v_0^2 + g^2 + hg \left(\frac{dg}{dt} - D_- v_N \right) \,. \tag{C.10}$$

To recover the same estimate of the continuum the last term must vanish. In the homogeneous case ($g = 0$), this is what happens. However, in general, in the inhomogeneous case ($g \neq 0$) the discrete estimate does not coincide with the continuum one. In [7] Olsson was able to prove that, with the additional assumption of analyticity of the data, the continuum estimate can be recovered. Most of the numerical experiments carried out in this dissertation, however, violate this requirement.

Note that at $t = 0$ we have that $\frac{dg}{dt} - D_- u_N = \mathcal{O}(h)$ and that, as shown in subsection 5.3.2, the semi-discrete approximation is convergent.

Vita

Gioel Calabrese was born on September 29th, 1974, in Parma, Italy, to an American mother and Italian father. Gioel was raised in Parma, living for the first 10 years of his life in Via Einstein. From an early age, Gioel enjoyed science and mathematics, and chose to study at a high school with a focus on science, where he would have the opportunity to explore this area further. Following high school, Gioel enrolled in physics at the University of Parma. In his fourth year of undergraduate studies, he participated in the Erasmus exchange program to attend the University of Erlangen-Nuremberg in Germany. Upon his return to Parma, he began independent research for his undergraduate thesis in classical general relativity under the guidance of Professors Massimo Pauri and Luca Lusanna and was awarded his laurea *magna cum laude* in February 1999.

It was in Germany that Gioel met his future wife, Pamela, a native of Southwest Scotland. The couple moved to the United States in late 1999, where Gioel began graduate studies in physics at the Pennsylvania State University, intending to specialize in theoretical relativity. Working with his advisor, Professor Jorge Pullin, he became increasingly interested in numerical relativity. Part of the Gravity Group transferred to Louisiana State University in late 2001, where Gioel continued with research towards his doctoral degree. Following the conferral of the degree of Doctor of Philosophy, Gioel plans to remain active in the field in an academic environment and looks forward to teaching and working as a member of the international numerical relativity community. Gioel enjoys traveling and spending time with his family.